UNSAM
ITeDA Instituto de Tecnologías en Detección y Astropartículas
KIT Karlsruher Institut für Technologie

Signal Processing in the Microwave SQUID Multiplexer-based Readout Systems for Magnetic Microbolometer Detector Arrays

Eng. Juan Manuel Salum

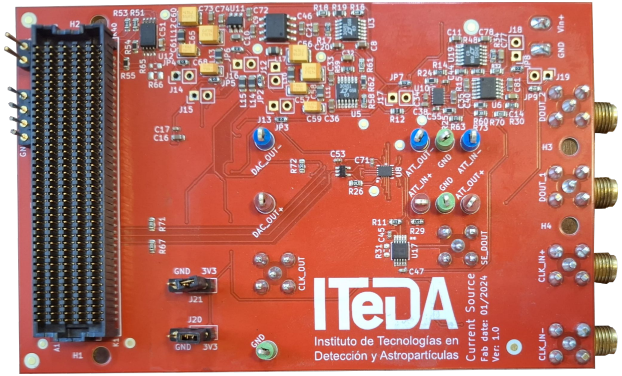

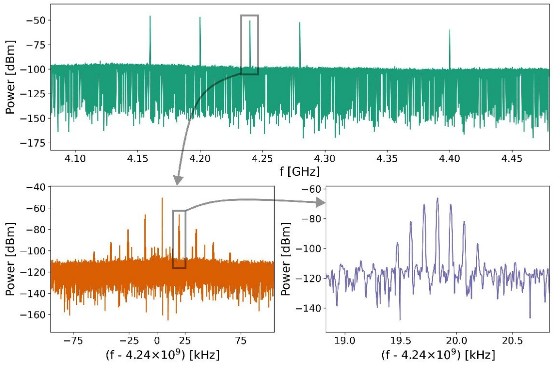

Motivation

Photons propagate freely

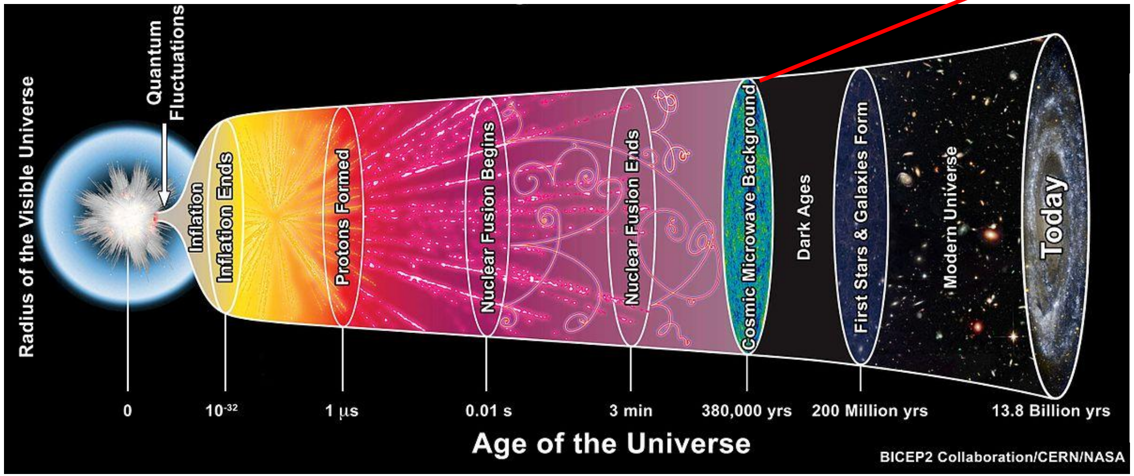

The Cosmic Microwave Background (CMB)

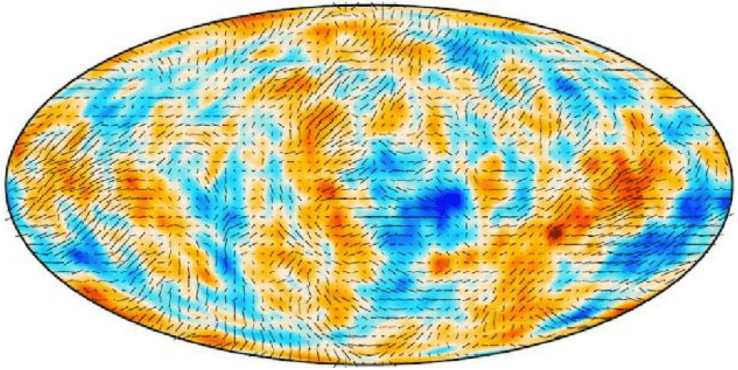

Credits: Planck collaboration

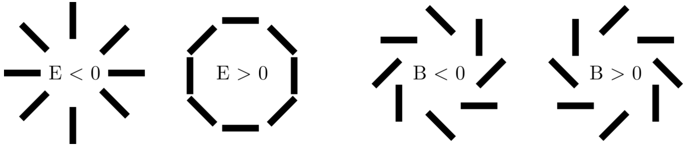

E modes *B modes*

Inflation Theory

- ➔ The Universe expanded exponentially, leading to its cooling
- ➔ Photons enabled to freely propagate after recombination epoch
- ➔ The footprint of this process is in the CMB polarization
- ➔ CMB is E- and B-mode polarized
- ➔ **Detecting B modes provides direct evidence of the inflationary period**

Challenges for B modes detection

PICO

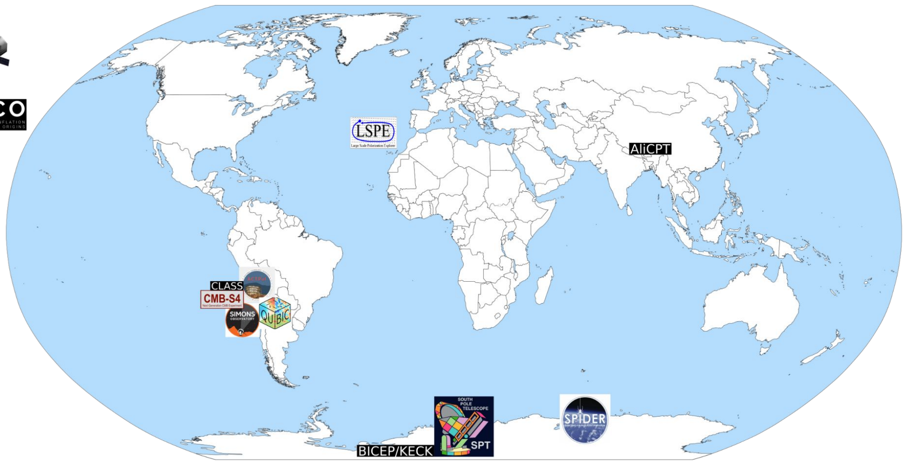

The CMB and foregrounds spectrum

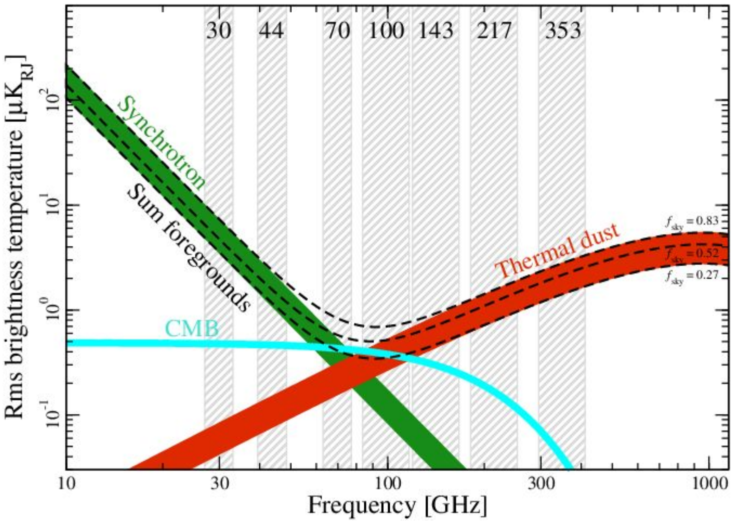

Credits: Planck collaboration

- ➔ Effort by the scientific community to detect the B-modes
- ➔ Measurement <u>challenges</u>:
  - ◆ <u>B-mode is a weak signal</u> ⟶ Low-temperature bolometer arrays
  - ◆ <u>Foregrounds</u> ⟶ Additional bands for foregrounds removal
  - ◆ <u>Systematic effects</u> ⟶ Calibration

Bolometric Interferometry

Q&U Bolometric Interferometer for Cosmology

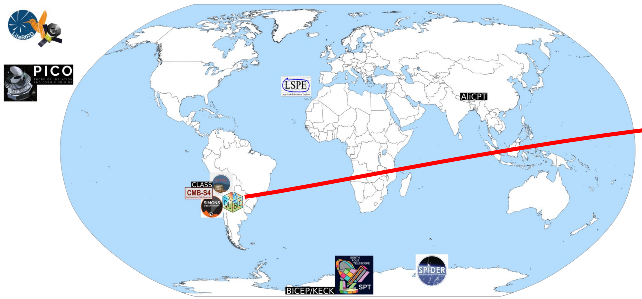

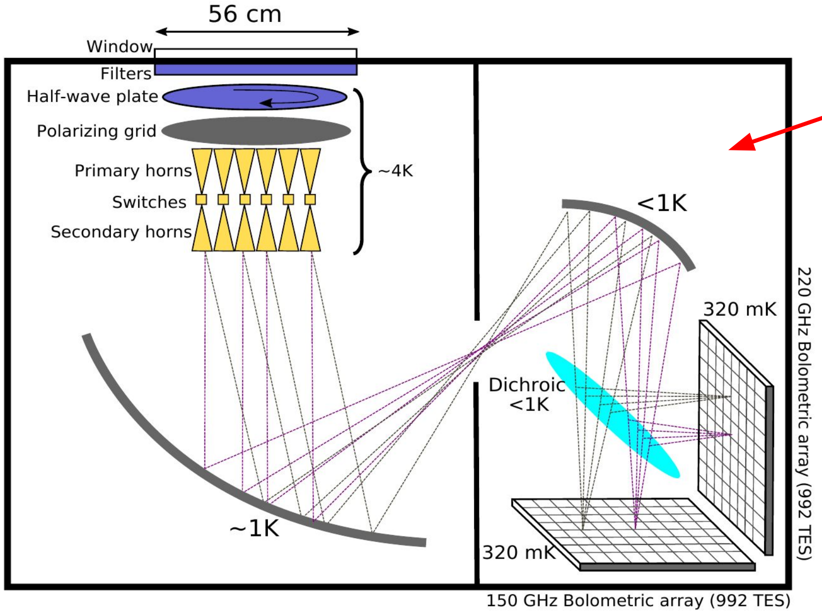

The QUBIC telescope

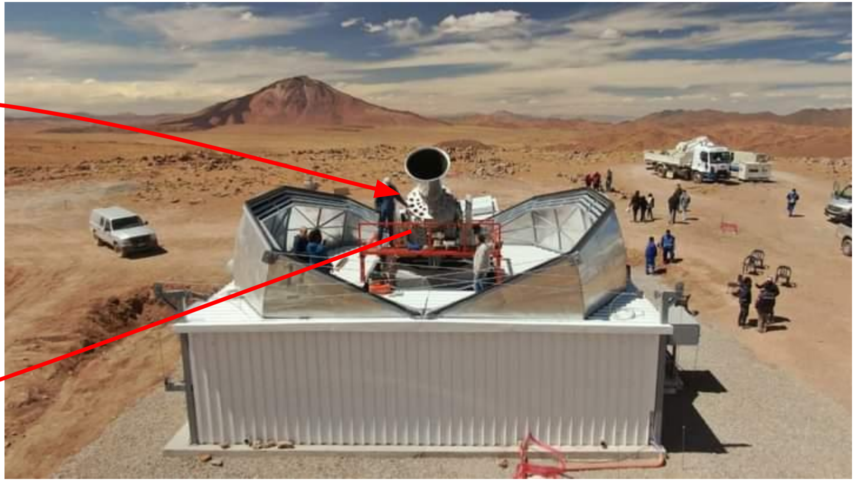

- ➔ QUBIC is the first bolometric interferometer for CMB
- ➔ 2048 bolometers for the 150GHz and 220GHz bands
- ➔ The system is housed in a cryostat
- ➔ QUBIC challenges:
  - ◆ **Designing the dichroic for simultaneous 150GHz and 220GHz operation**
  - ◆ **Readout system scalability**

A proposal for QUBIC next generation

- ➔ Multichroic antenna-coupled Magnetic Microbolometer (MMB)
  - ◆ Multiple observation bands in a single pixel avoid the use of the dichroic
  - ◆ Novel detector based on the Magnetic Microcalorimeter (MMC)

- ➔ A microwave SQUID multiplexer readout system
  - ◆ Promising technology for high-sensitivity readout
  - ◆ High-multiplexing factor

- ➔ Room temperature electronics
  - ◆ A system based on a software-defined radio scheme is proposed due to its adaptability to different experiments requirements
  - ◆ FPGA-based system enables high scalability and flexibility

A proposal for QUBIC next generation

- ➔ Multichroic antenna-coupled Magnetic Microbolometer (MMB)
  - ◆ Multiple observation bands in a single pixel avoid the use of the dichroic
  - ◆ Novel detector based on the Magnetic Microcalorimeter (MMC)

- ➔ A microwave SQUID multiplexer readout system
  - ◆ Promising technology for high-sensitivity readout
  - ◆ High-multiplexing factor

- ➔ Room temperature electronics
  - ◆ A system based on a software-defined radio scheme is proposed due to its adaptability to different experiments requirements
  - ◆ FPGA-based system enables high scalability and flexibility

Novel detector: Magnetic Microbolometer (MMB)

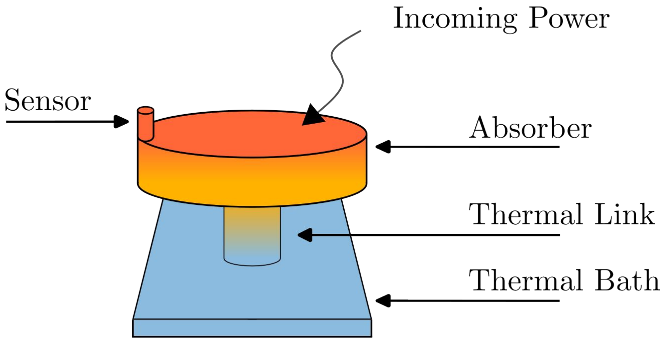

- ➔ Photons absorption increase the absorber temperature
- ➔ Au:Er paramagnetic sensor embedded in a magnetic field changes its magnetization with the temperature
- ➔ The magnetic flux passing through the sensor changes, generating a measurable signal

MMB readout

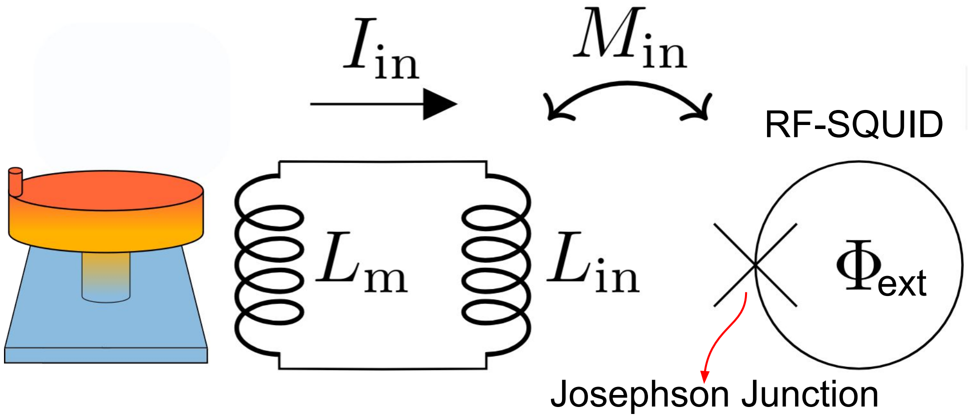

- ➔ Magnetic flux is read out with a radio frequency Superconducting Quantum Interference Device
- ➔ The supercurrent in the RF-SQUID follows

$$I_{\mathrm{s}} = -I_{\mathrm{c}} \sin\left(\frac{2\pi\Phi_{\mathrm{ext}}}{\Phi_0} + \frac{2\pi L_{\mathrm{s}} I_{\mathrm{s}}}{\Phi_0}\right)$$

Detector Signal

RF-SQUID readout

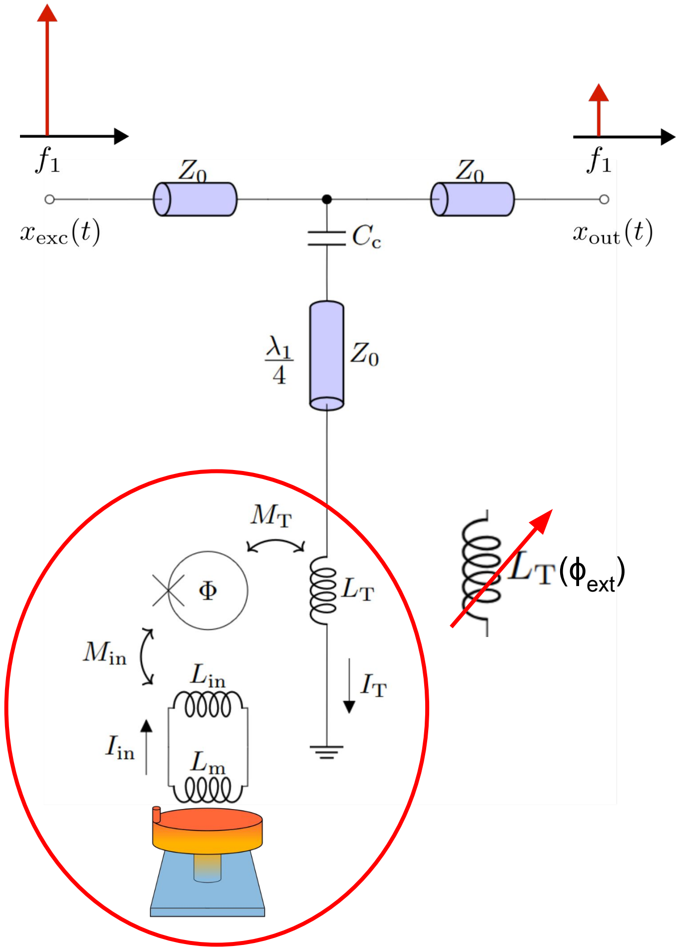

➔ RF-SQUID coupled to a resonator
➔ This forms a variable inductance with the SQUID signal

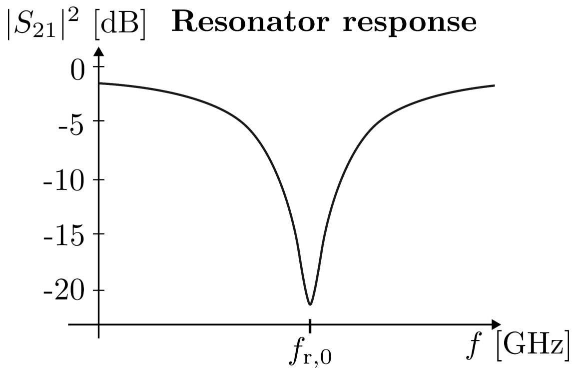

RF-SQUID readout

- ➔ RF-SQUID coupled to a resonator
- ➔ This forms a variable inductance with the SQUID signal
- ➔ Detector signal shifts the resonator response (s_{21})
- ➔ **A readout tone monitors the resonator state**

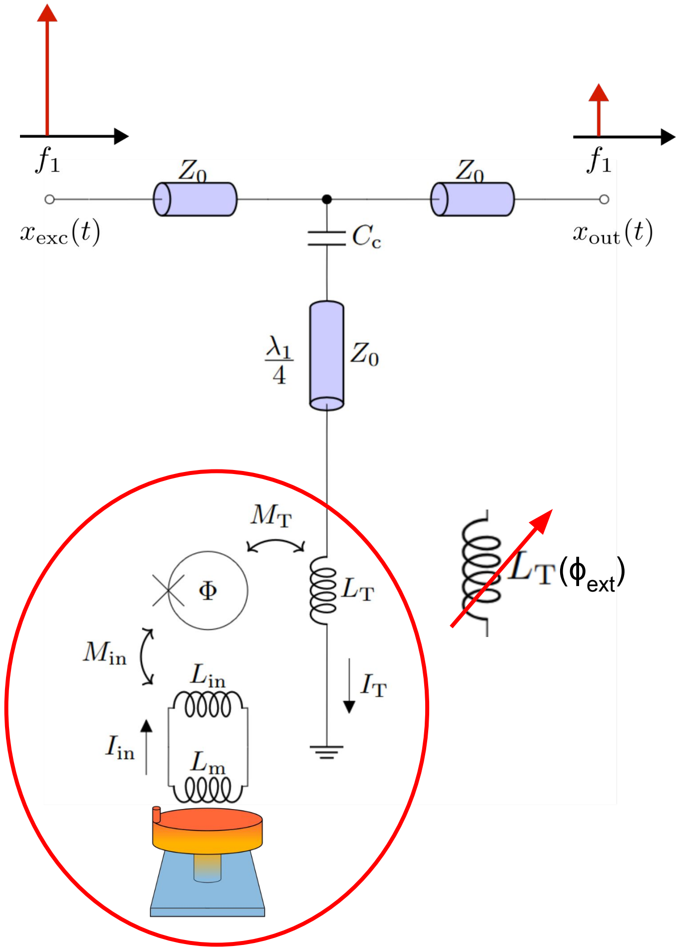

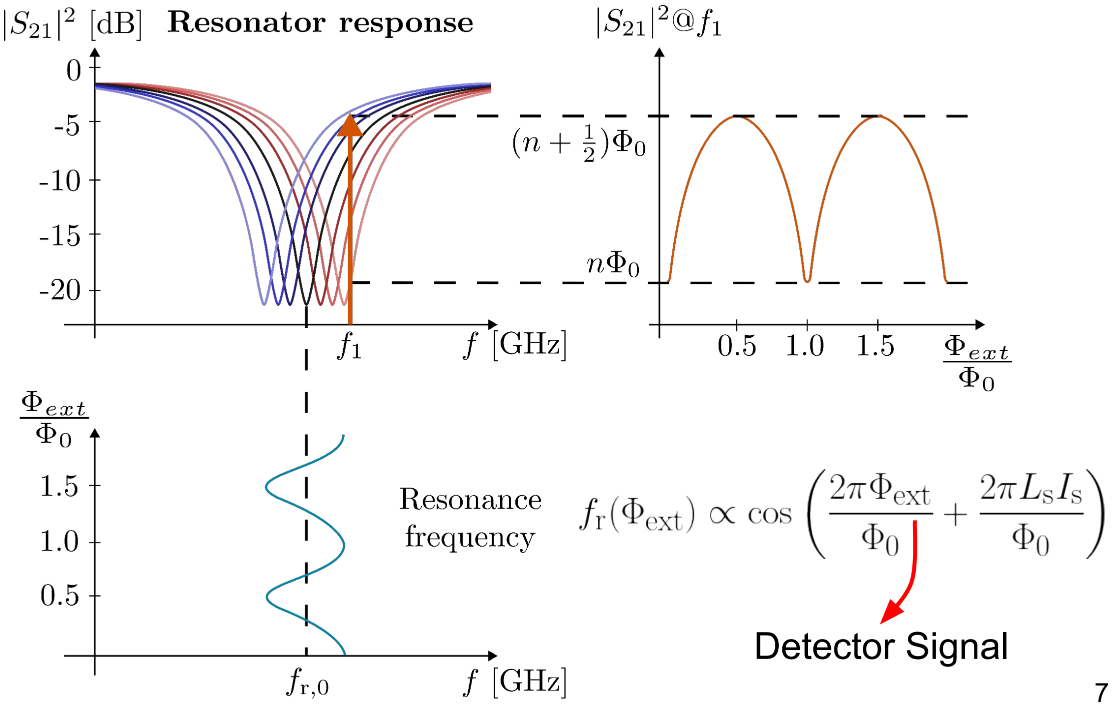

The Microwave SQUID Multiplexer (µMUX)

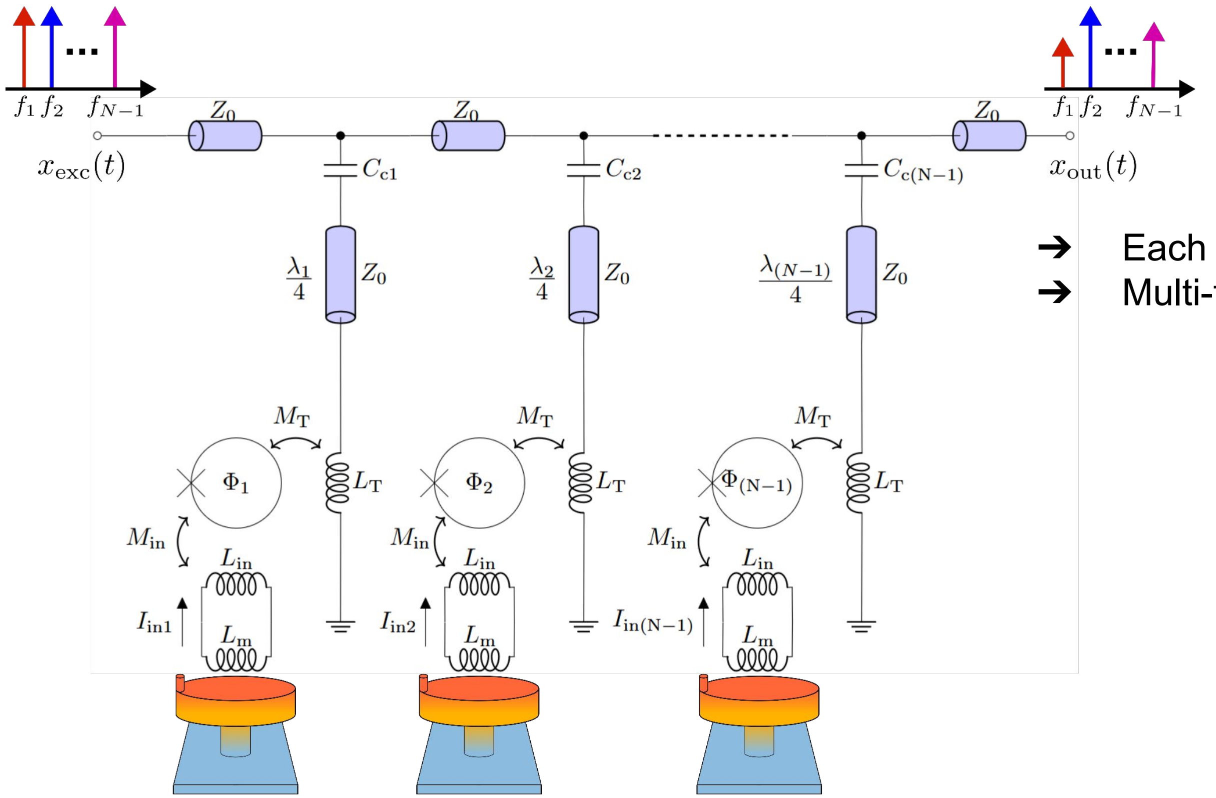

➔ Each channel is set to a unique frequency
➔ Multi-tonal signal monitors all channels

The Microwave SQUID Multiplexer (µMUX)

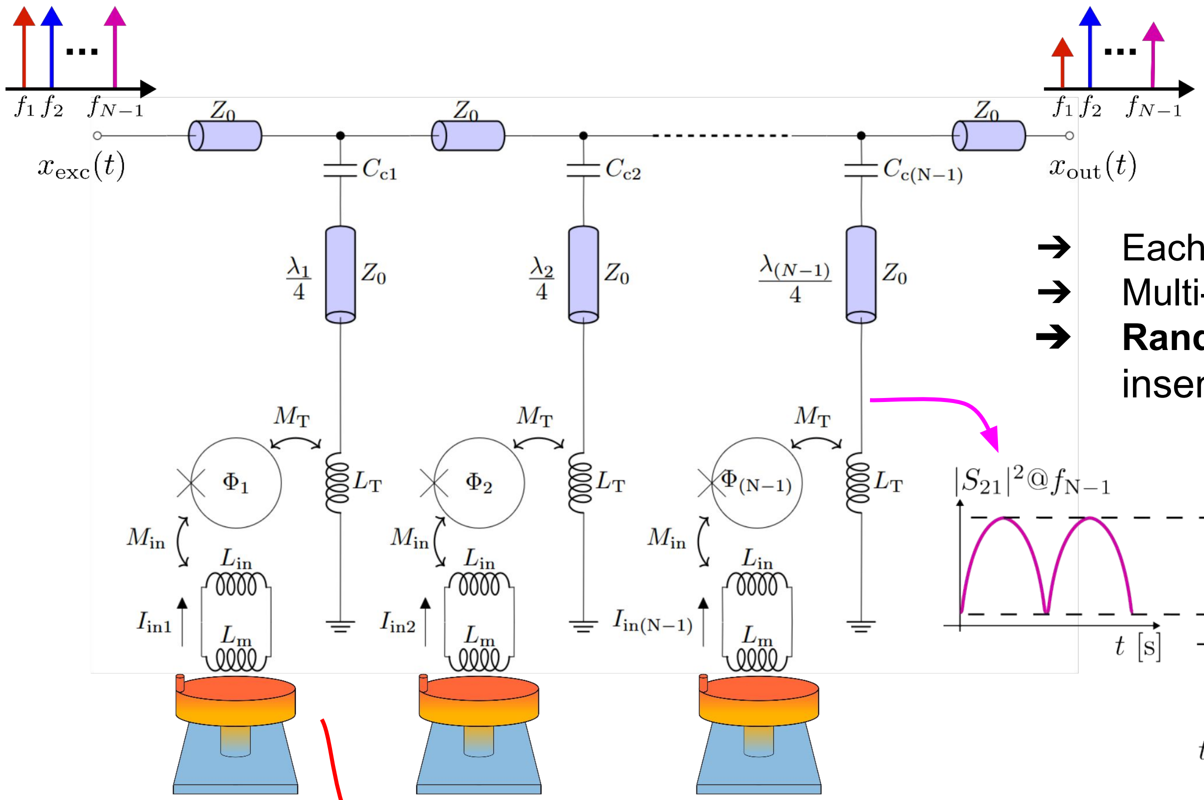

- ➔ Each channel is set to a unique frequency
- ➔ Multi-tonal signal monitors all channels
- ➔ **Random external flux problem:** insensitive SQUIDs

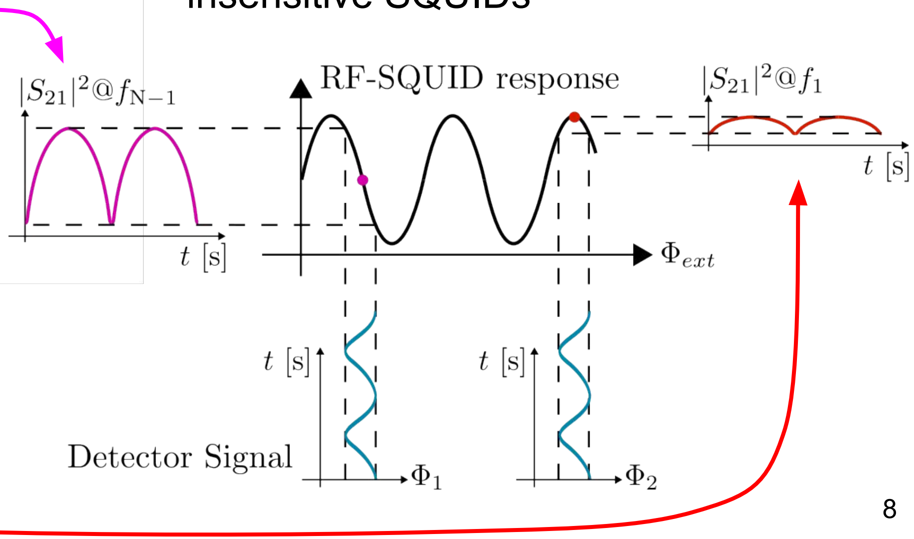

The µMUX: Fluxramp modulation

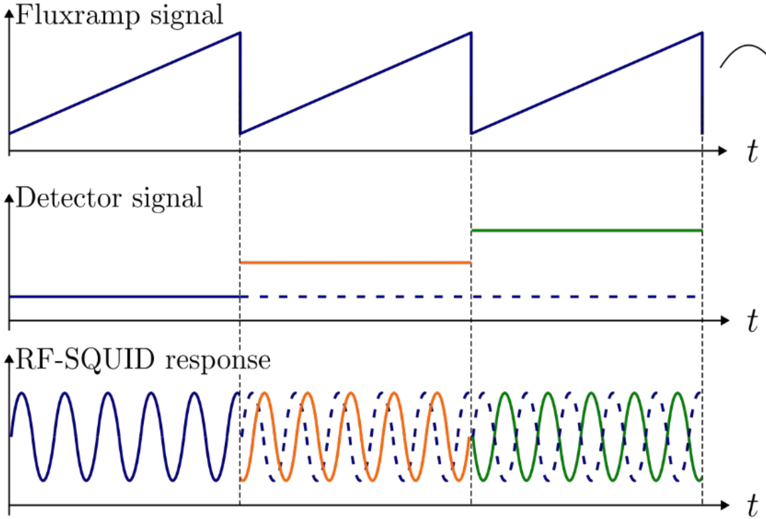

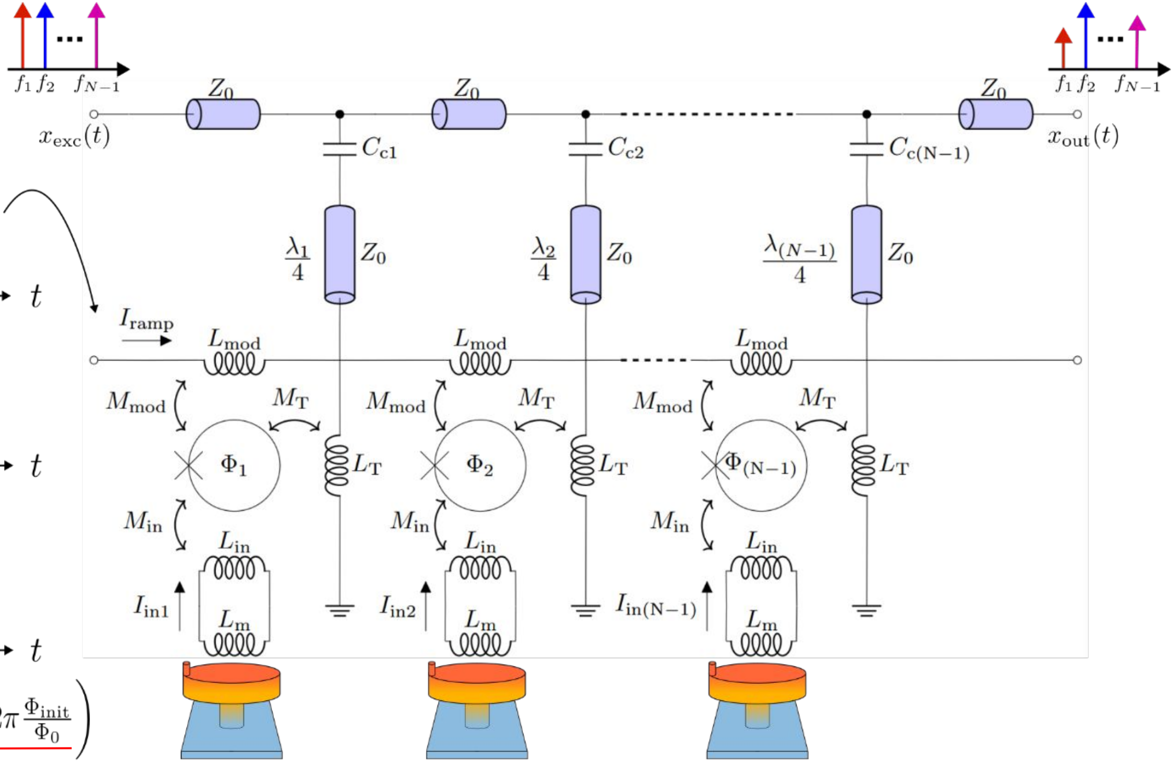

$$f_{\mathrm{r}}(\Phi_{\mathrm{ext}}) \propto \cos\left(2\pi \frac{I_{\mathrm{ramp}} M_{\mathrm{mod}} f_{\mathrm{ramp}}}{\Phi_0} t + 2\pi \frac{\Phi_{\mathrm{det}}}{\Phi_0} + 2\pi \frac{L_{\mathrm{S}} I_{\mathrm{S}}}{\Phi_0} + 2\pi \frac{\Phi_{\mathrm{init}}}{\Phi_0}\right)$$

Fluxramp Signal

Random Phase

Detector Signal

- ➔ A sawtooth signal is coupled to all the RF-SQUIDs
- ➔ The detector signal modulates the SQUID response's phase
- ➔ **Phase demodulation is required**

Software-defined radio scheme

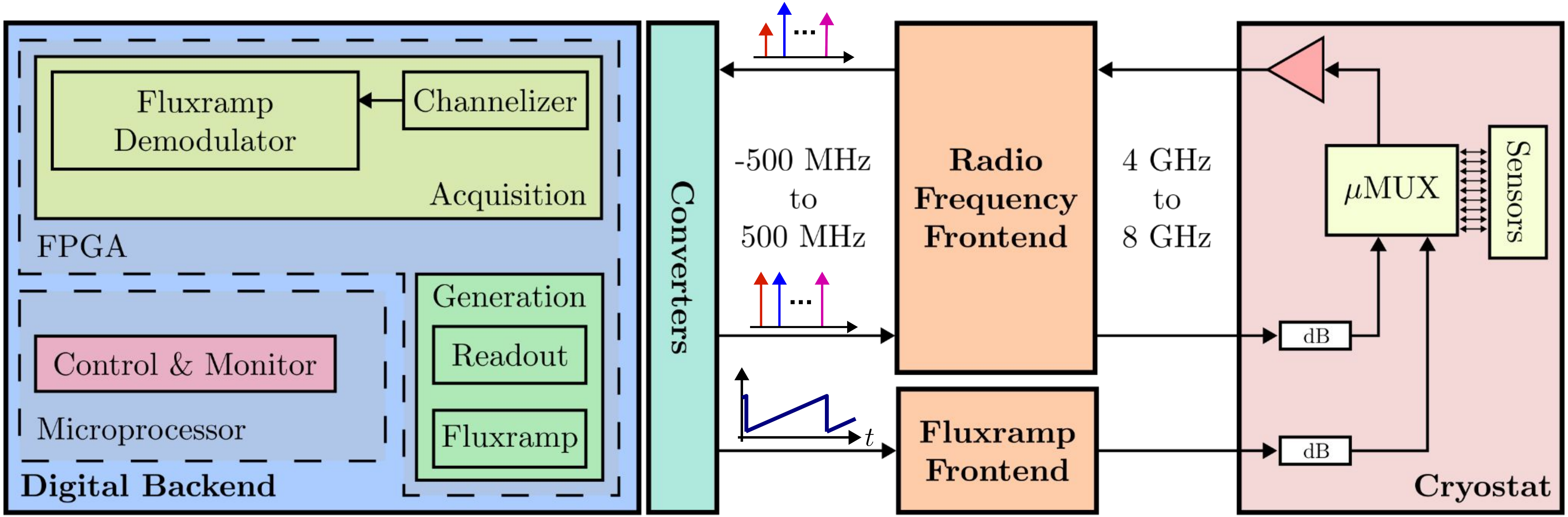

- ➔ Digital fluxramp and multi-tonal readout signals generation
- ➔ Conversion of readout and flux ramp signals to the analog domain
- ➔ Readout and fluxramp signals conditioning
- ➔ Readout signal acquisition and processing
  - ◆ Channelizer: readout tones separation and rf-SQUID recovery
  - ◆ Fluxramp demodulator: extract detector signals

Software-defined radio scheme

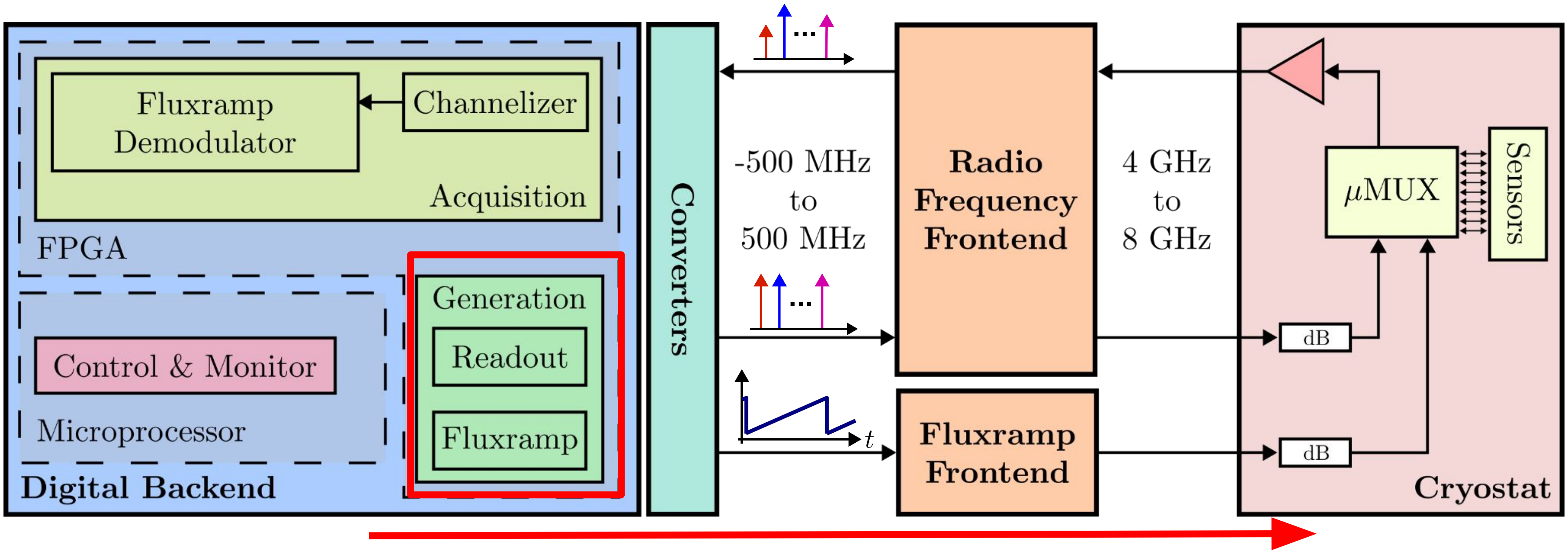

- ➔ Digital fluxramp and multi-tonal readout signals generation
- ➔ Conversion of readout and flux ramp signals to the analog domain
- ➔ Readout and fluxramp signals conditioning
- ➔ Readout signal acquisition and processing
  - ◆ Channelizer: readout tones separation and rf-SQUID recovery
  - ◆ Fluxramp demodulator: extract detector signals

Software-defined radio scheme

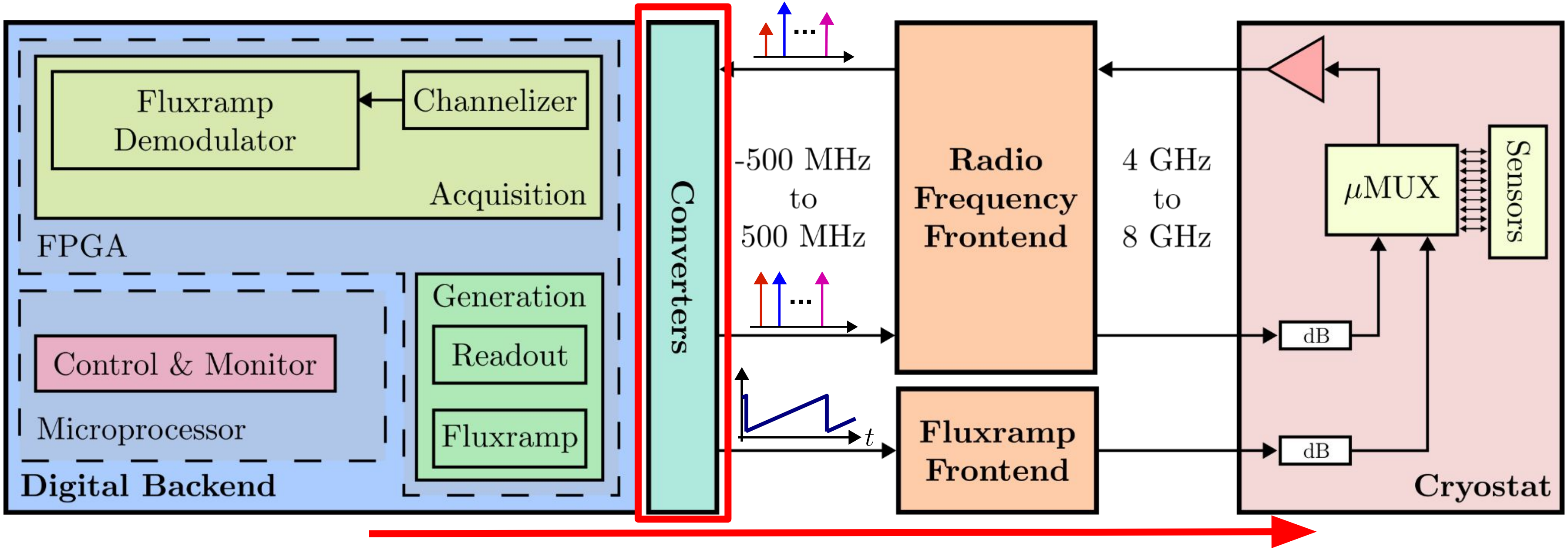

- ➔ Digital fluxramp and multi-tonal readout signals generation
- ➔ Conversion of readout and flux ramp signals to the analog domain
- ➔ Readout and fluxramp signals conditioning
- ➔ Readout signal acquisition and processing
  - ◆ Channelizer: readout tones separation and rf-SQUID recovery
  - ◆ Fluxramp demodulator: extract detector signals

Software-defined radio scheme

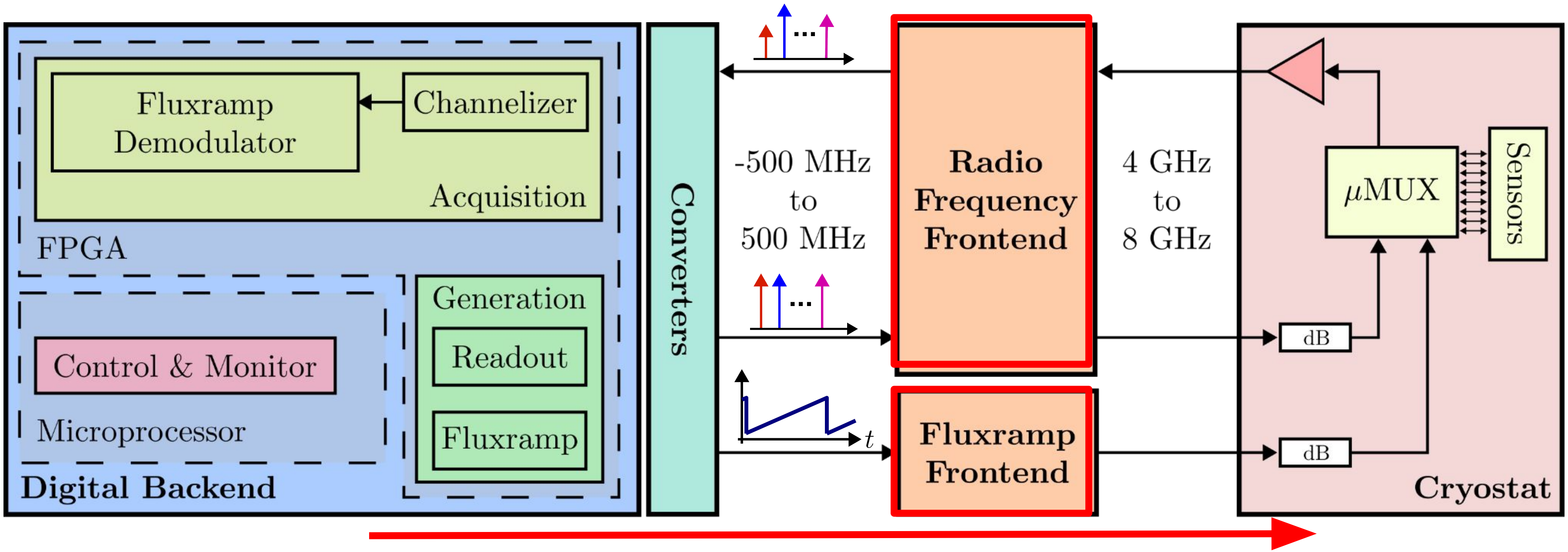

- ➔ Digital fluxramp and multi-tonal readout signals generation
- ➔ Conversion of readout and flux ramp signals to the analog domain
- ➔ Readout and fluxramp signals conditioning
- ➔ Readout signal acquisition and processing
  - ◆ Channelizer: readout tones separation and rf-SQUID recovery
  - ◆ Fluxramp demodulator: extract detector signals

Software-defined radio scheme

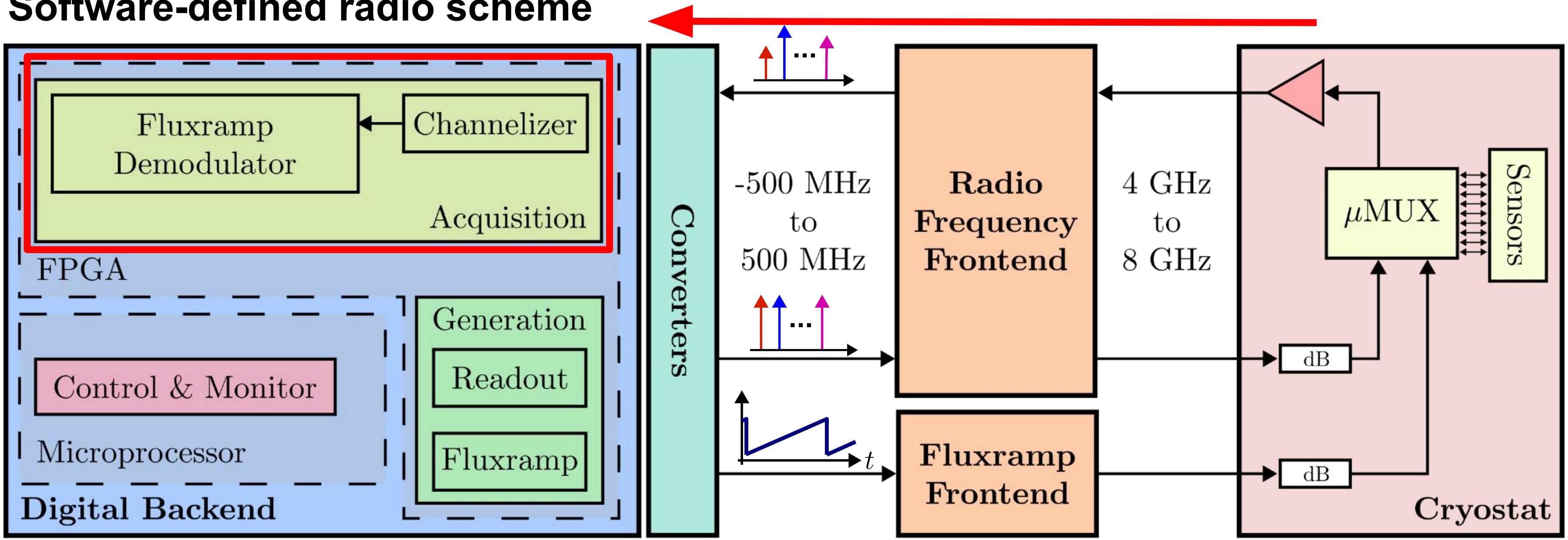

- ➔ Digital fluxramp and multi-tonal readout signals generation
- ➔ Conversion of readout and flux ramp signals to the analog domain
- ➔ Readout and fluxramp signals conditioning
- ➔ Readout signal acquisition and processing
  - ◆ Channelizer: readout tones separation and rf-SQUID recovery
  - ◆ Fluxramp demodulator: extract detector signals

This work objectives

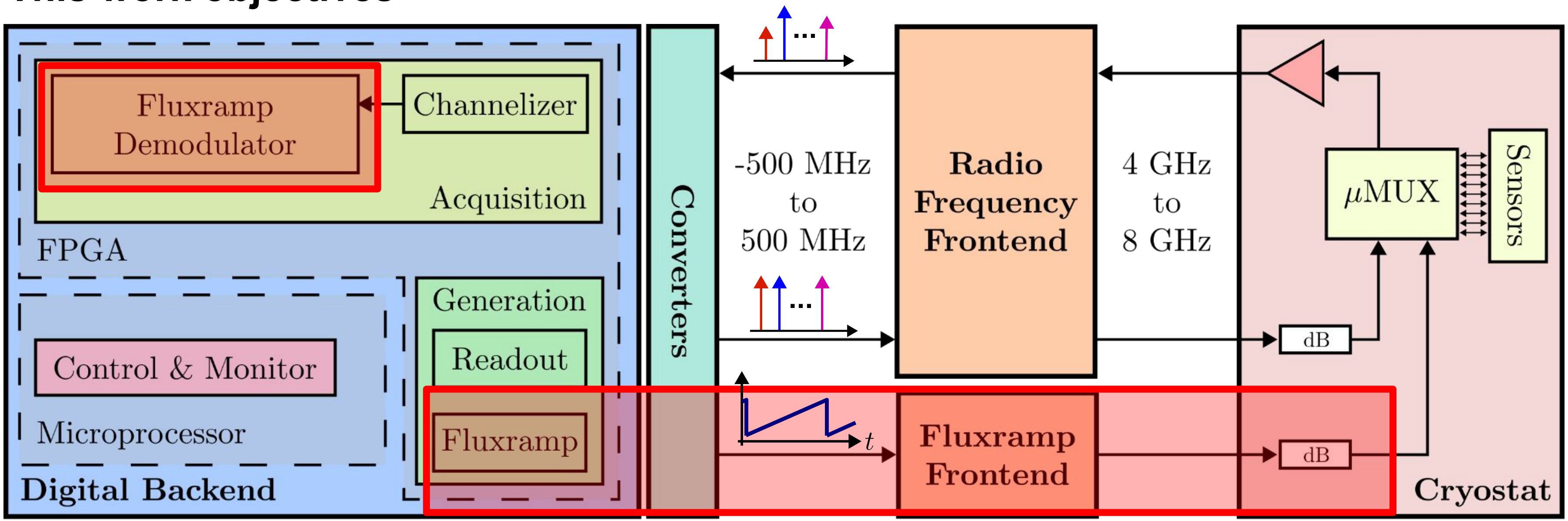

- ➔ Generation sub-system
  - ◆ **Fluxramp signal chain design**
  - ◆ **Integrate the signal generation sub-system**
- ➔ Processing sub-system
  - ◆ **Multi-channel demodulator**
  - ◆ **Acquisition chain integration**
- ➔ **Readout System Validation**

Fluxramp signal noise requirement

- ➔ Background noise > Detector noise > Readout noise
- ➔ Background Limited Photometry (BLIP) condition achieved from 0.045 Hz to 760 Hz

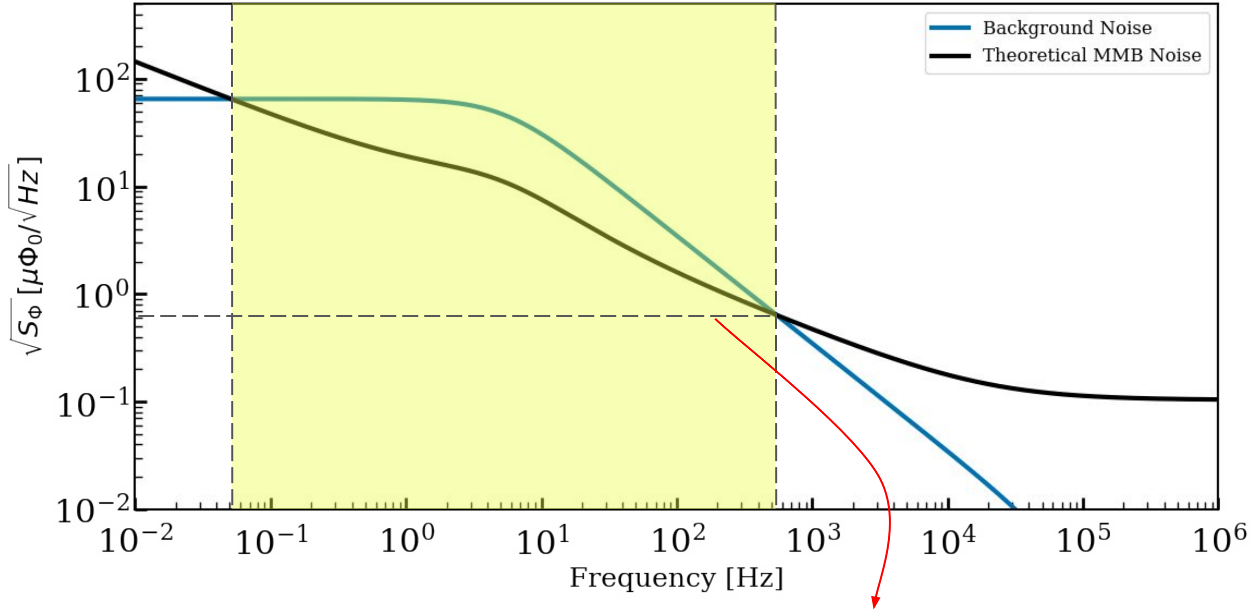

- ➔ **Fluxramp noise much less than 0.6$\mu\phi_0/\sqrt{Hz}$**

Fluxramp frontend and cryogenic setup

➔ Modulation Signal Synthesizer (MSS) around the 16 bits DAC MAX5891

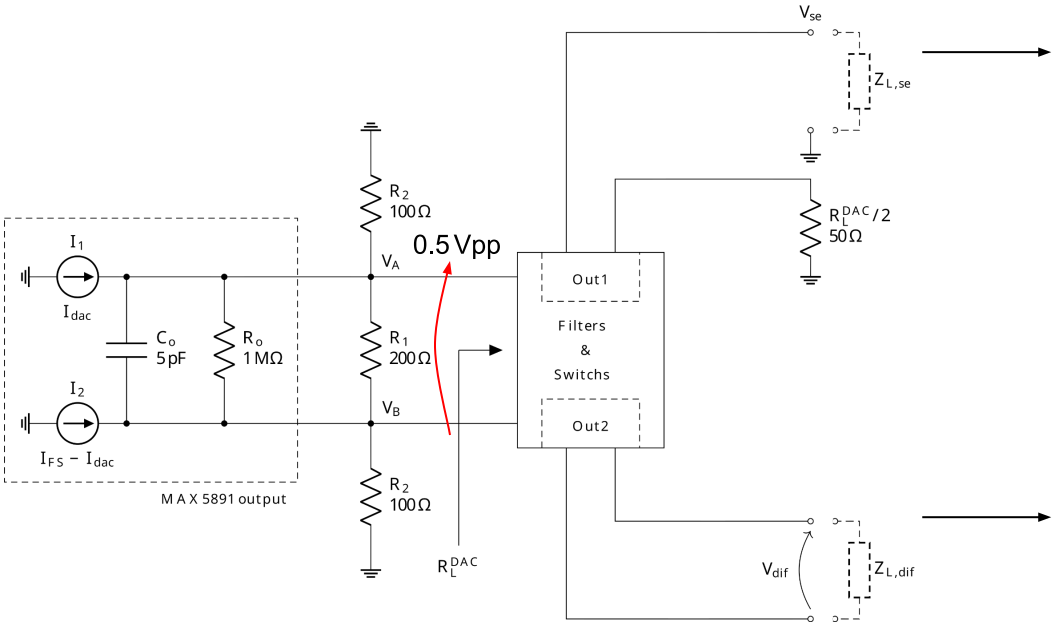

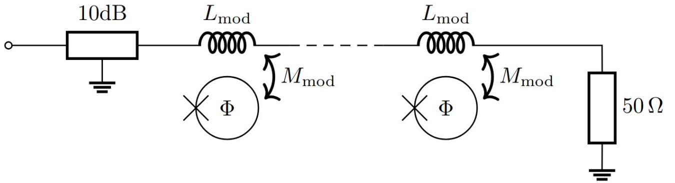

Cryogenic single-ended setup

Cryogenic differential setup

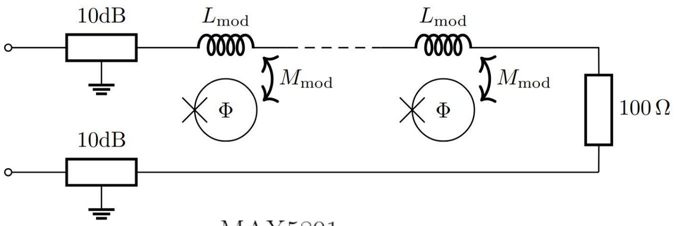

➔ Theoretical noise spectral density $S_{\mathrm{MAX5891}}\Big|_{\mathrm{dBm}} = 1\,\mathrm{dBm} - \mathrm{SNR}_{\mathrm{dB}} - 10\log_{10}\left(\frac{f_s^{\mathrm{MAX5891}}}{2}\right) = -164\frac{\mathrm{dBm}}{\mathrm{Hz}}$

20 mA full scale current in a double-terminated 100 Ω load

10 MHz clock signal

➔ 10 dB attenuation reduces fluxramp noise

MSS board: Noise analysis

Modulation line coupling (M_{mod} = 2291 ϕ_0/A)

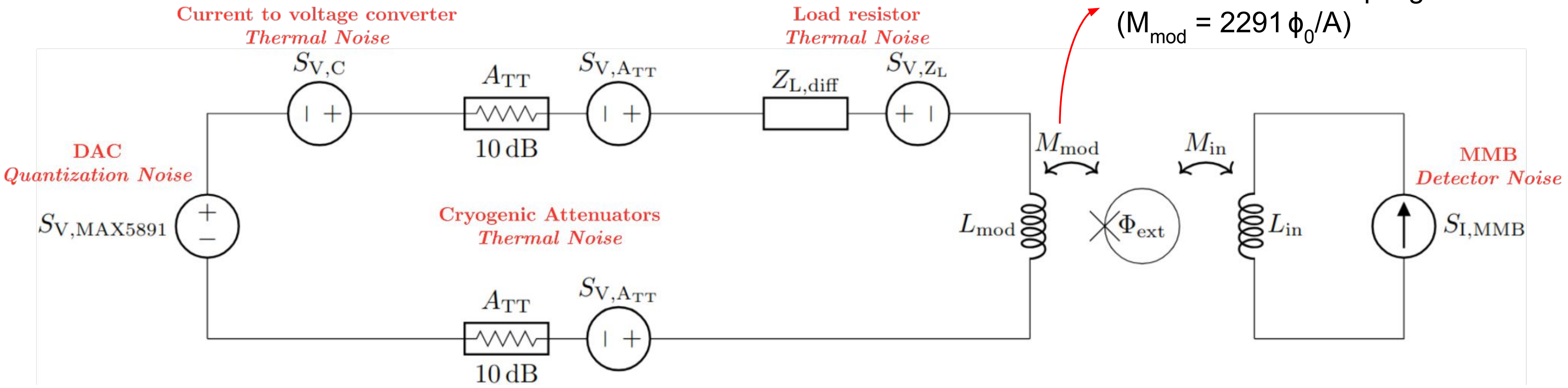

Source	Flux Noise Spectral Density [$\mu\phi_0/\sqrt{Hz}$]
DAC quantized noise	0.015
Current to voltage circuit	0.005
Cryogenic attenuator	0.001
100 Ω load	0.004
Total MSS Noise	0.016
Expected MMB Noise	0.6

Expected MMB signal degraded by 0.034 %

Generation sub-system integration

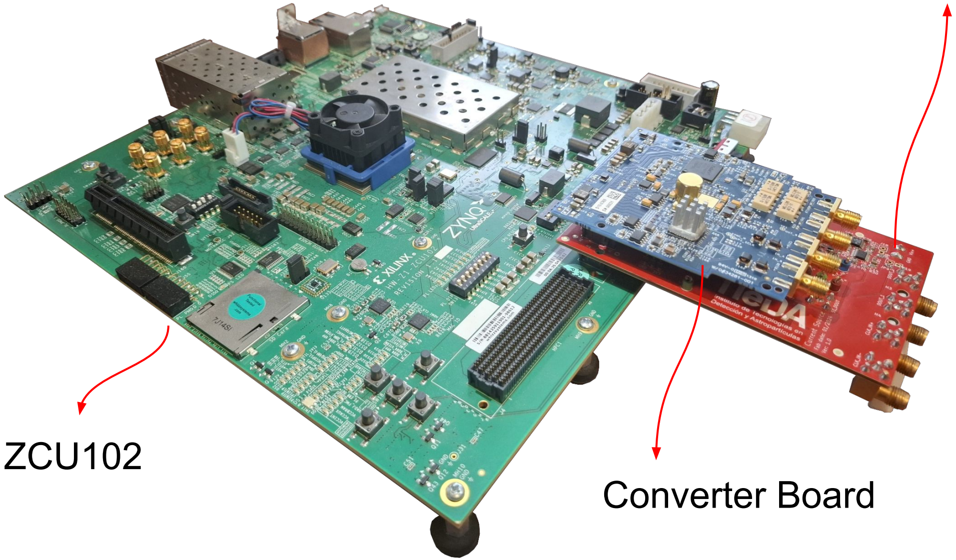

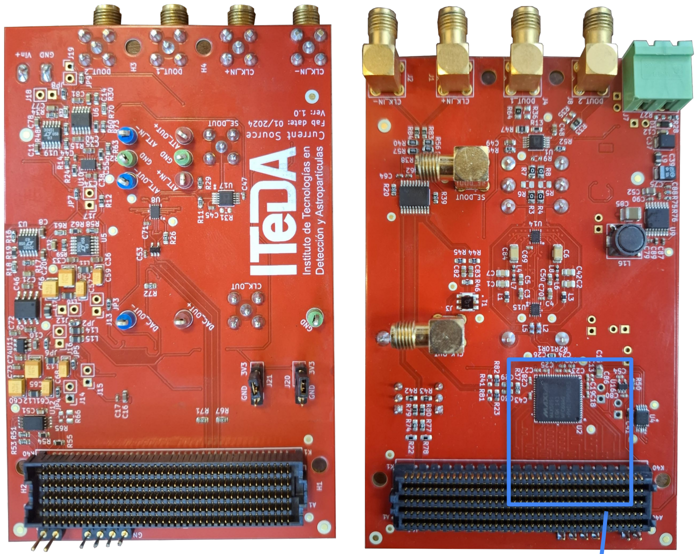

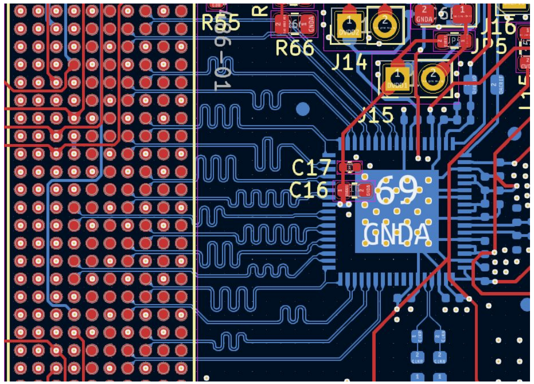

- ➔ Stackable board system (ZCU102-MSS-Converter board)
  - ◆ Back-to-back FMC+ connector
  - ◆ Via-in-pad for high-density routing
- ➔ Digital Fluxramp generation
  - ◆ dual-port BRAM
  - ◆ 16 differential microstrip transmission lines

MSS characterization

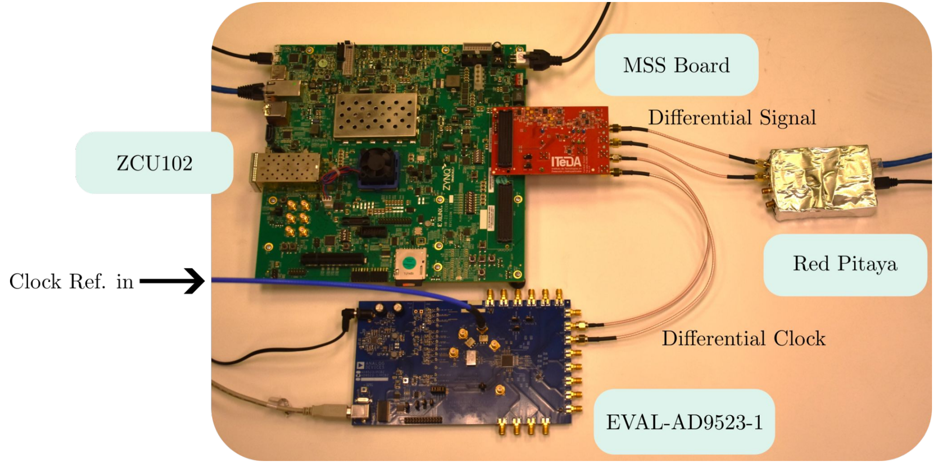

- ➔ Clock generated by the EVAL-AD9523-1 board
- ➔ Signal acquisition using Red Pitaya
- ➔ 200 Hz to 100 kHz signal generation
- ➔ Total Harmonic Distortion (THD) and Spurious Free Dynamic Range (SFDR) characterization
- ➔ THD < 0.02 % and SFDR=80 dBc consistent with the manufacturer's specifications

Baseline MSS noise < Expected MMB noise

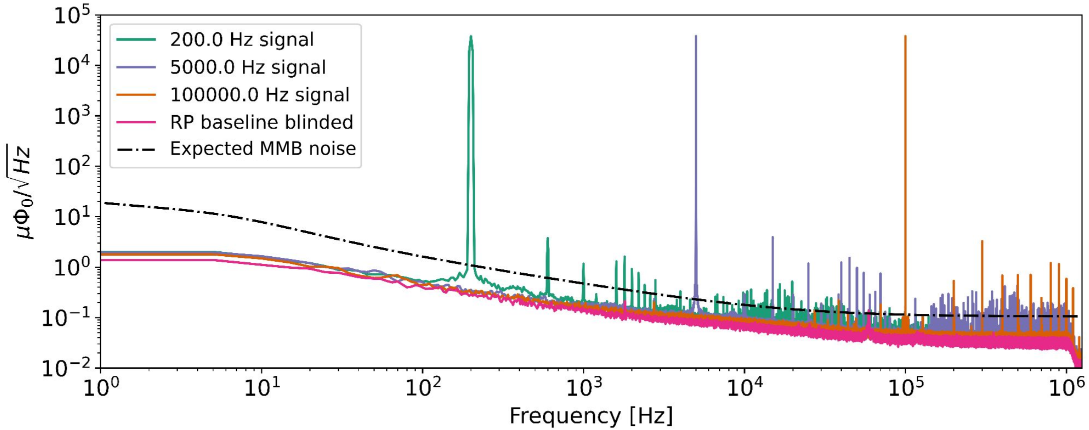

Fluxramp demodulator

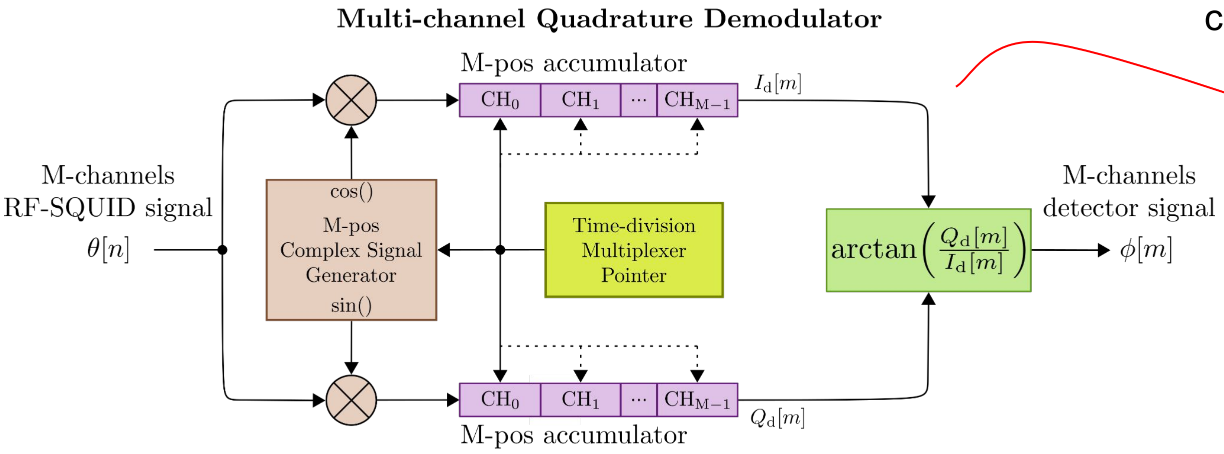

Typically implementation for a single channel demodulation as

$$\phi[m] = \arctan\left(-\frac{\sum_{n=0}^{N-1} \theta[n] \sin(\Omega_{\mathrm{mod}} n)}{\sum_{n=0}^{N-1} \theta[n] \cos(\Omega_{\mathrm{mod}} n)} \right)$$

Average Filter

- ➔ Correlation method with a complex exponential at the RF-SQUID frequency
- ➔ A low-pass filter removes the high-frequency components of mixing
- ➔ Arctangent function returns the input signal phase
- ➔ Time-division Multiplexing (TDM) enables multiple input signals demodulation
- ➔ **Filter and TDM implemented as a moving average filter in an M-position accumulator**

System nonlinearity

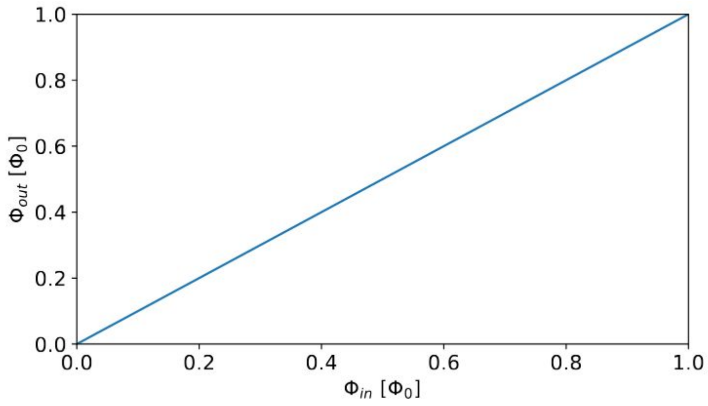

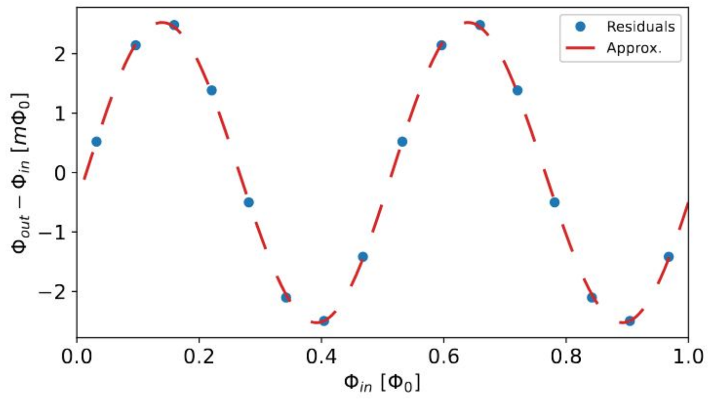

- ➔ Many groups reported non-linearities in the readout system
- ➔ Detector signal simulated as a linear signal
- ➔ Residuals observed after the demodulator output
- ➔ **Conclusion: the demodulator produces undesired components that aliases to the detector band**

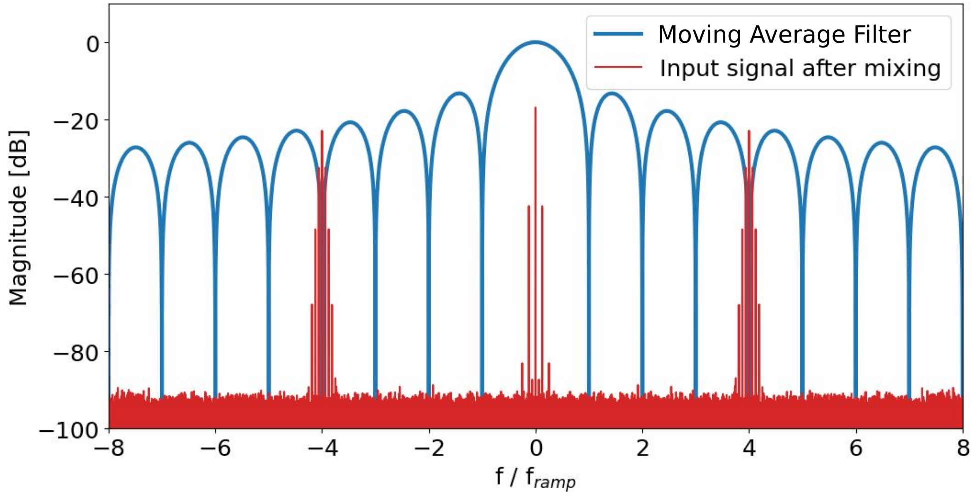

Salum et al., 2023, 10.1007/s10909-023-02993-z

Weighted filter implementation

$$\phi[m] = \arctan\left(-\frac{\sum_{n=0}^{N-1} \theta[n]\ \sin(\Omega_{mod} n) W[n]}{\sum_{n=0}^{N-1} \theta[n]\ \cos(\Omega_{mod} n) W[n]}\right)$$

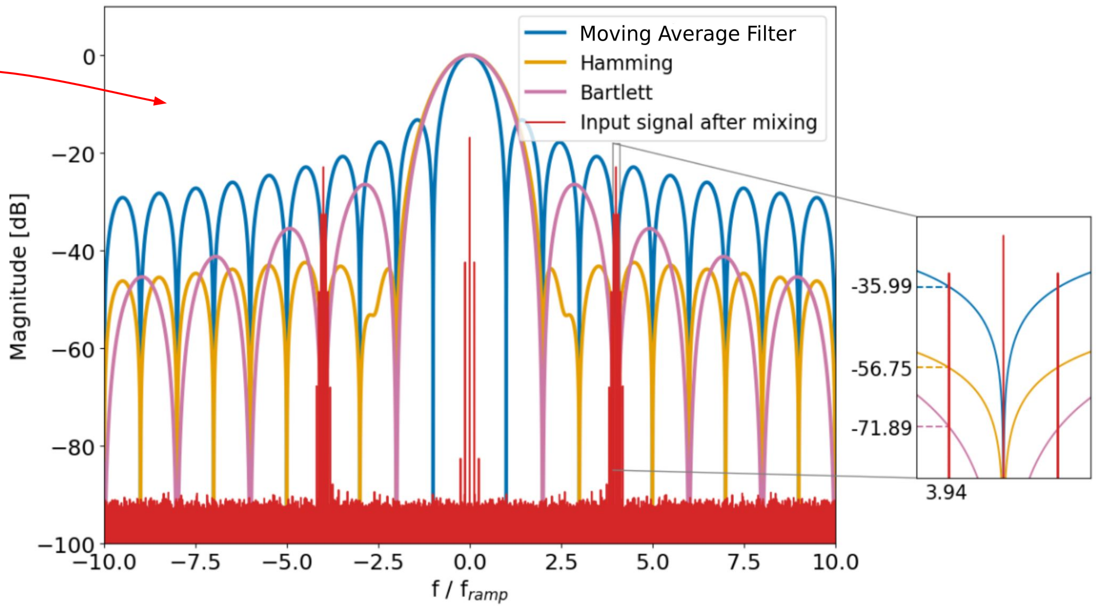

➔ Adding a window function improves the attenuation

➔ An improvement of **more than 35dB** achieved with the Bartlett window

Salum et al., 2023, 10.1007/s10909-023-02993-z

System scalability challenge

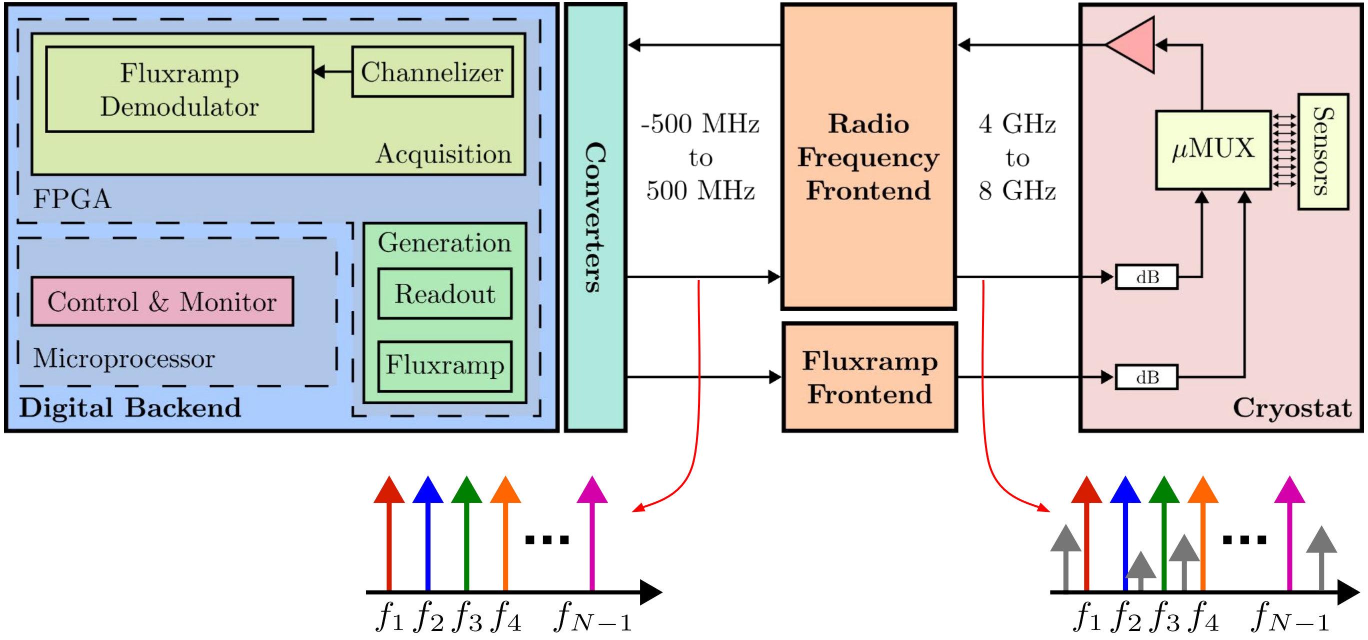

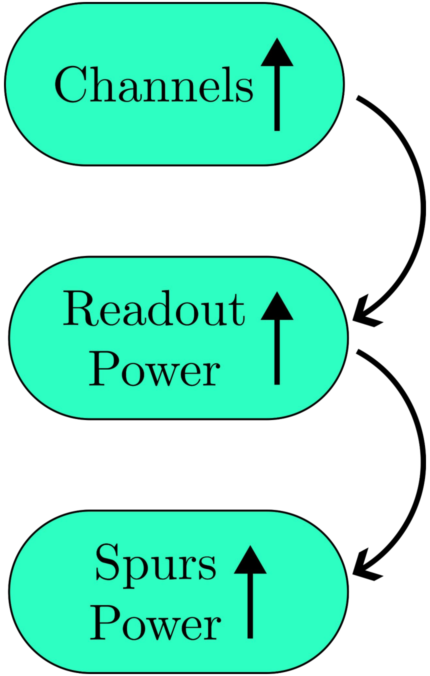

➔ State-of-the-art systems face scalability problems

➔ Higher readout power increases spurs power due to RF devices nonlinearities

➔ **Proposed: *Spectral engineering* for multi-channel dynamic performance optimization**

Salum et al., 2024, 10.1007/s10909-024-03049-6

Spectral Engineering

Typical phase modulated rf-SQUID response

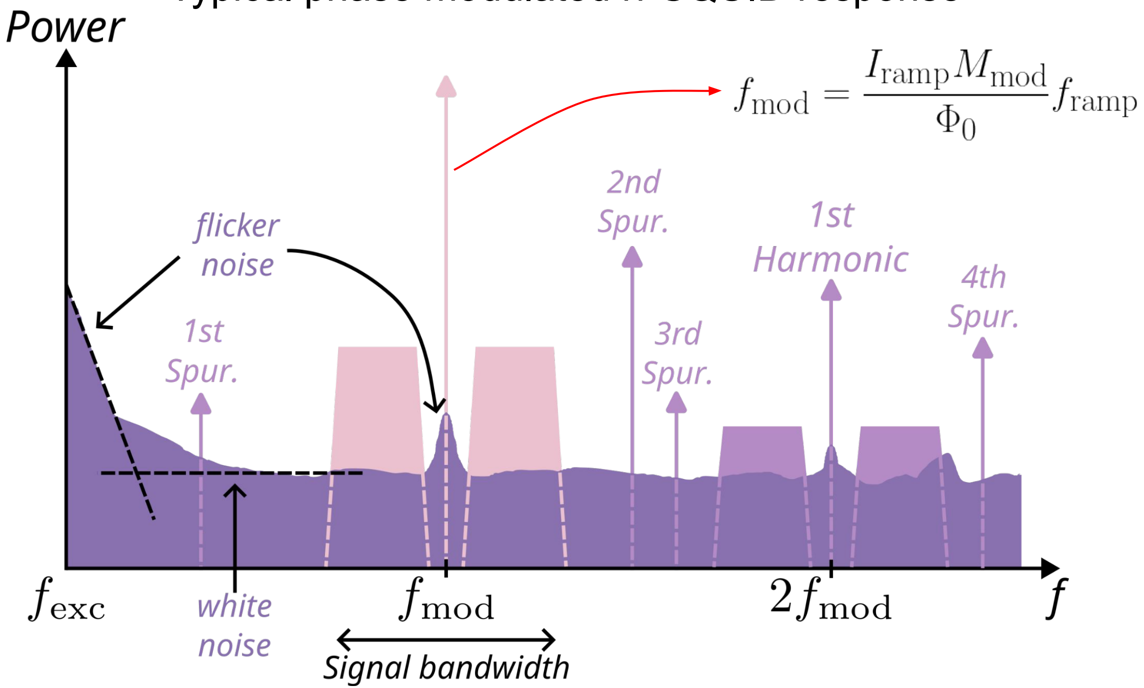

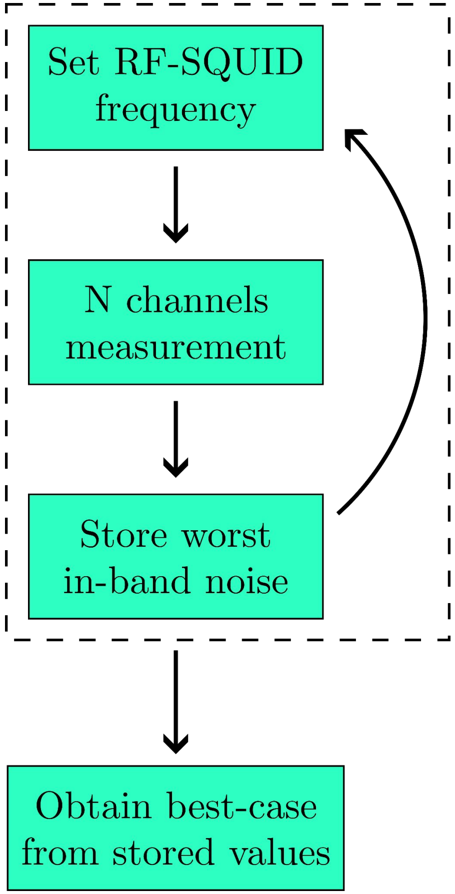

This technique achieves a 50 dB improvement between the best and worst in-band noise powers

Salum et al., 2024, 10.1007/s10909-024-03049-6

Microwave SQUID Multiplexer characterization

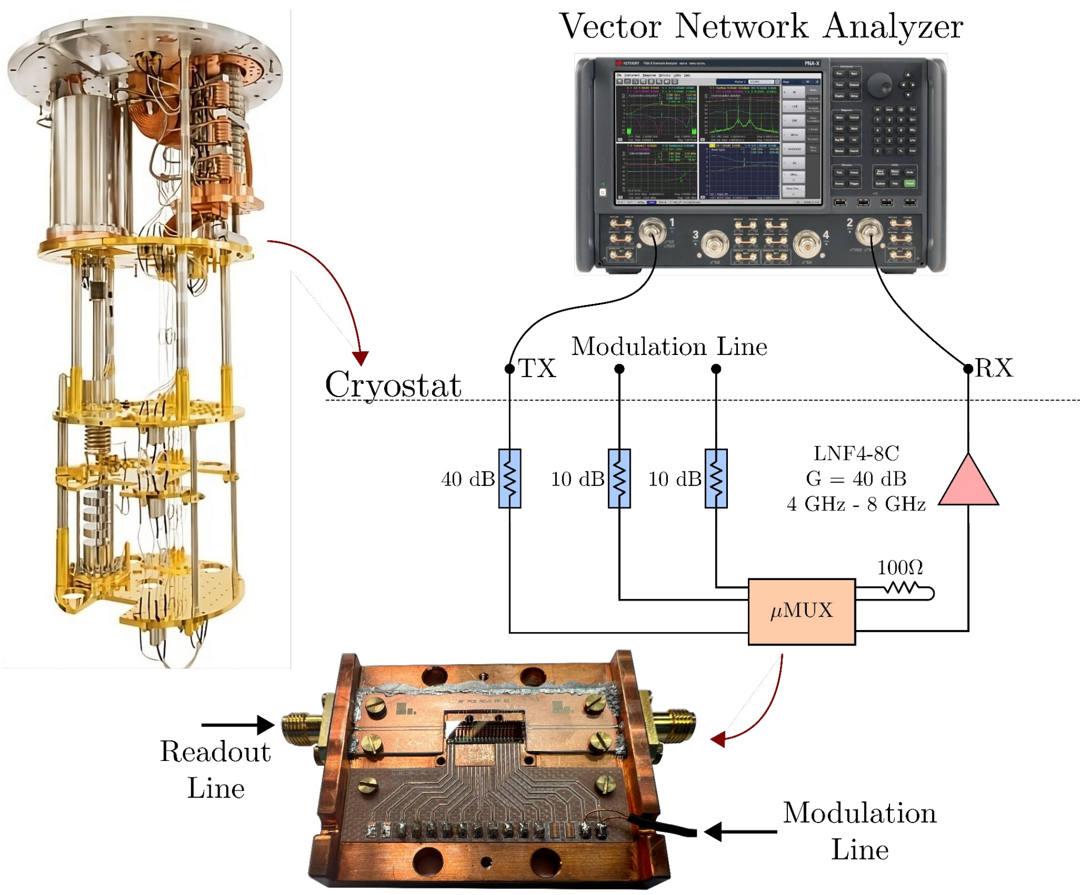

Microwave SQUID Multiplexer

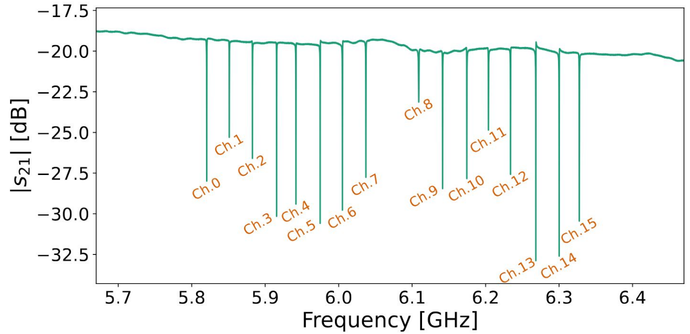

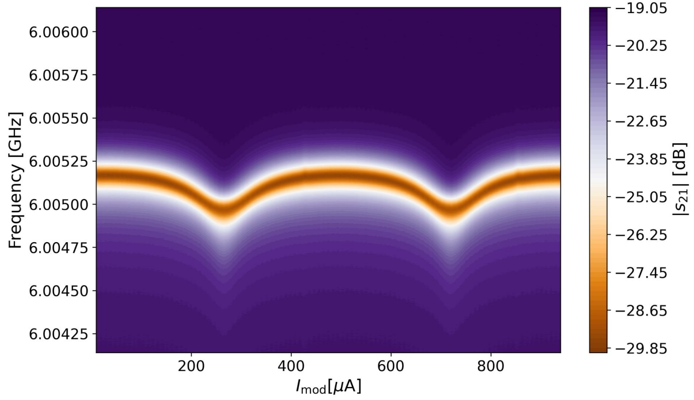

➔ Obtained channel parameters:
- Resonance frequencies
- Bandwidths
- Transmission depths
- M_{mod}

System integration

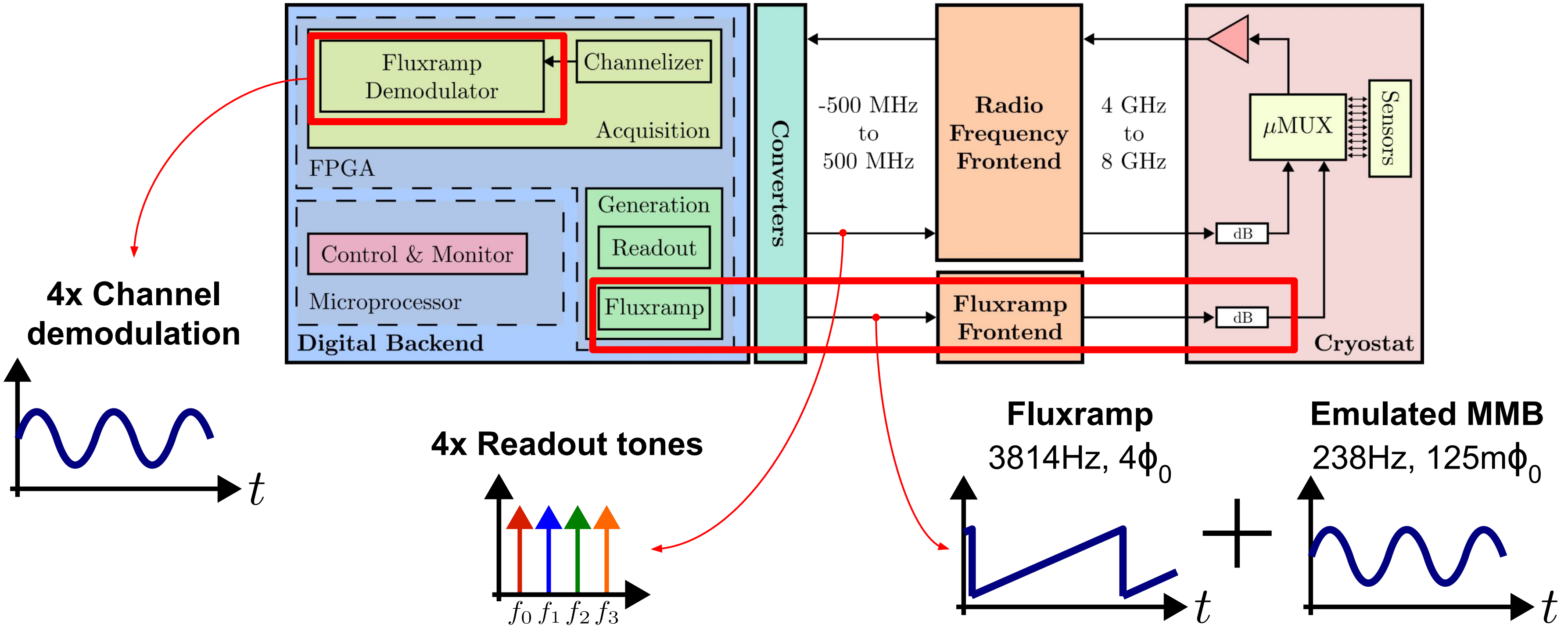

➔ Fluxramp demodulator integrated with a 4-channel Channelizer.

➔ Complete readout assembly

➔ A 238 Hz, 125 mϕ_0 MMB signal was emulated (added to the modulation signal in the BRAM)

System validation

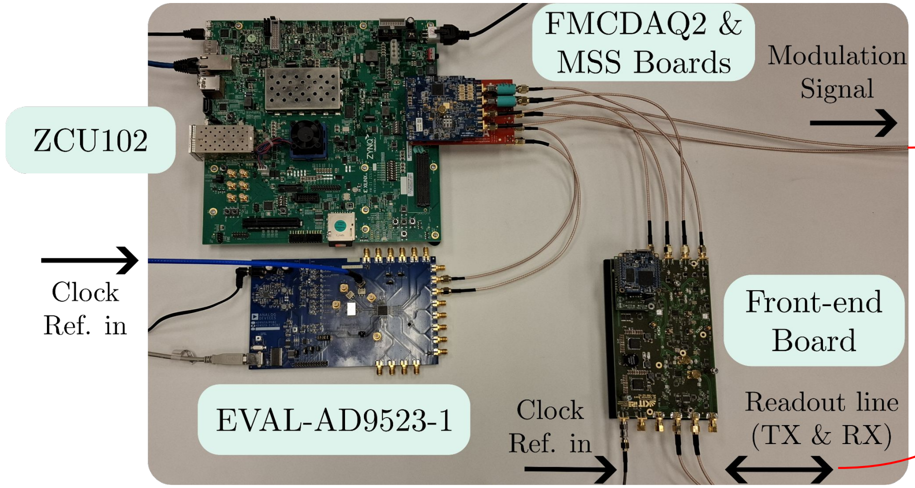

Fluxramp

3814Hz, $4\phi_0$

Emulated MMB

238Hz, $125m\phi_0$

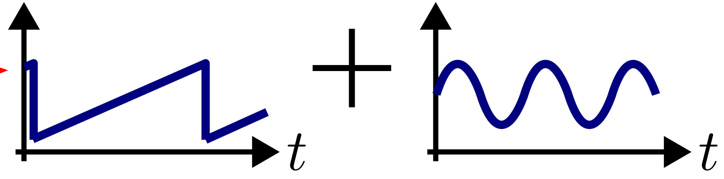

Readout tones

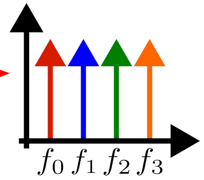

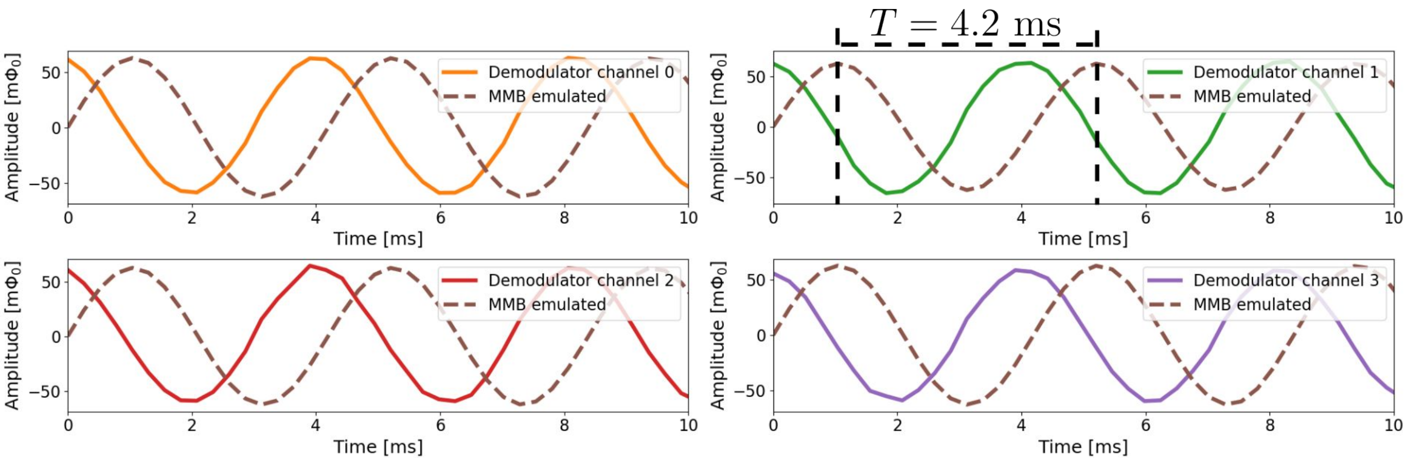

Successful readout system validation

Summary

- ✓ **The readout system was successfully integrated and validated**
- ✓ **The fluxramp system meets the noise requirements** for Magnetic Microbolometer detectors readout
- ✓ **The source of the system's nonlinearity was explained and a solution was proposed**
- ✓ The proposed **Spectral Engineering technique, successfully overcomes the noise vs. spur trade-off**, achieving improvements of up to 50 dB

<u>This work established a foundation for future Magnetic Microbolometer readout</u>

Back-up

QUBIC current readout

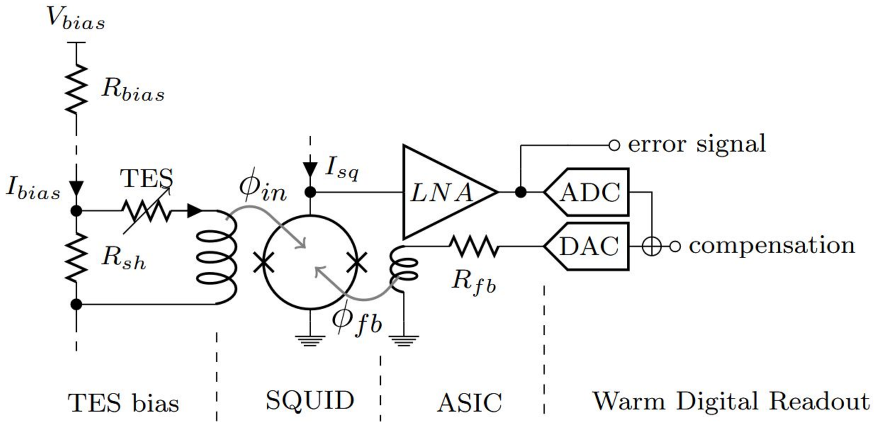

Single pixel readout

128 to 1 time-division multiplexer system

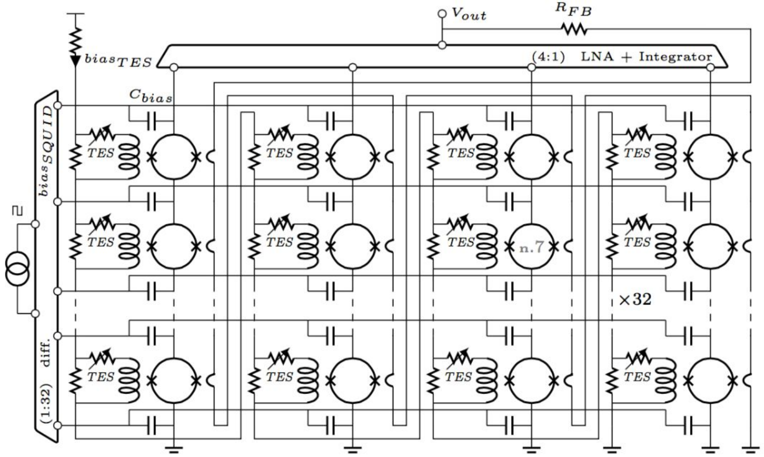

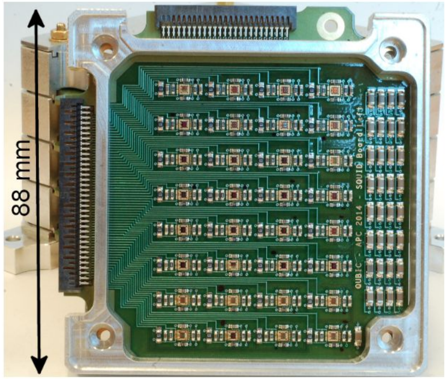

Multichroic antenna-coupled Magnetic Microbolometer

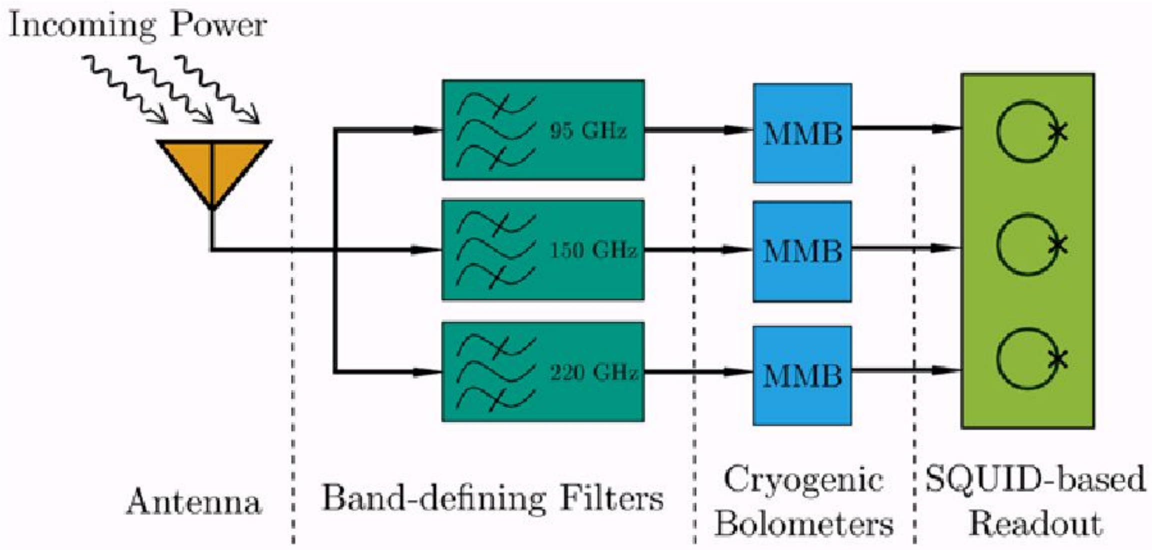

Josephson Junction

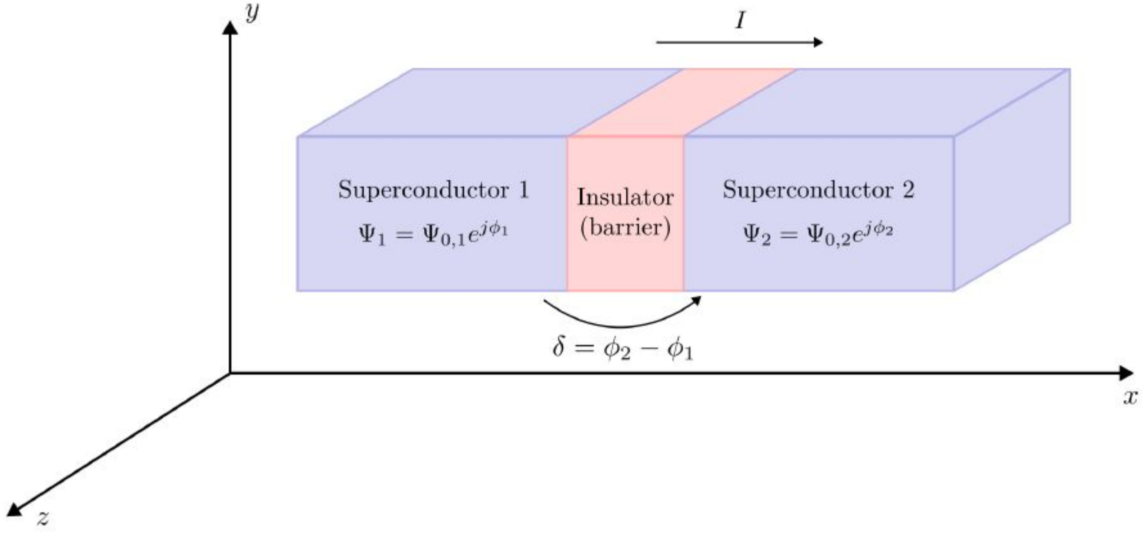

Readout system

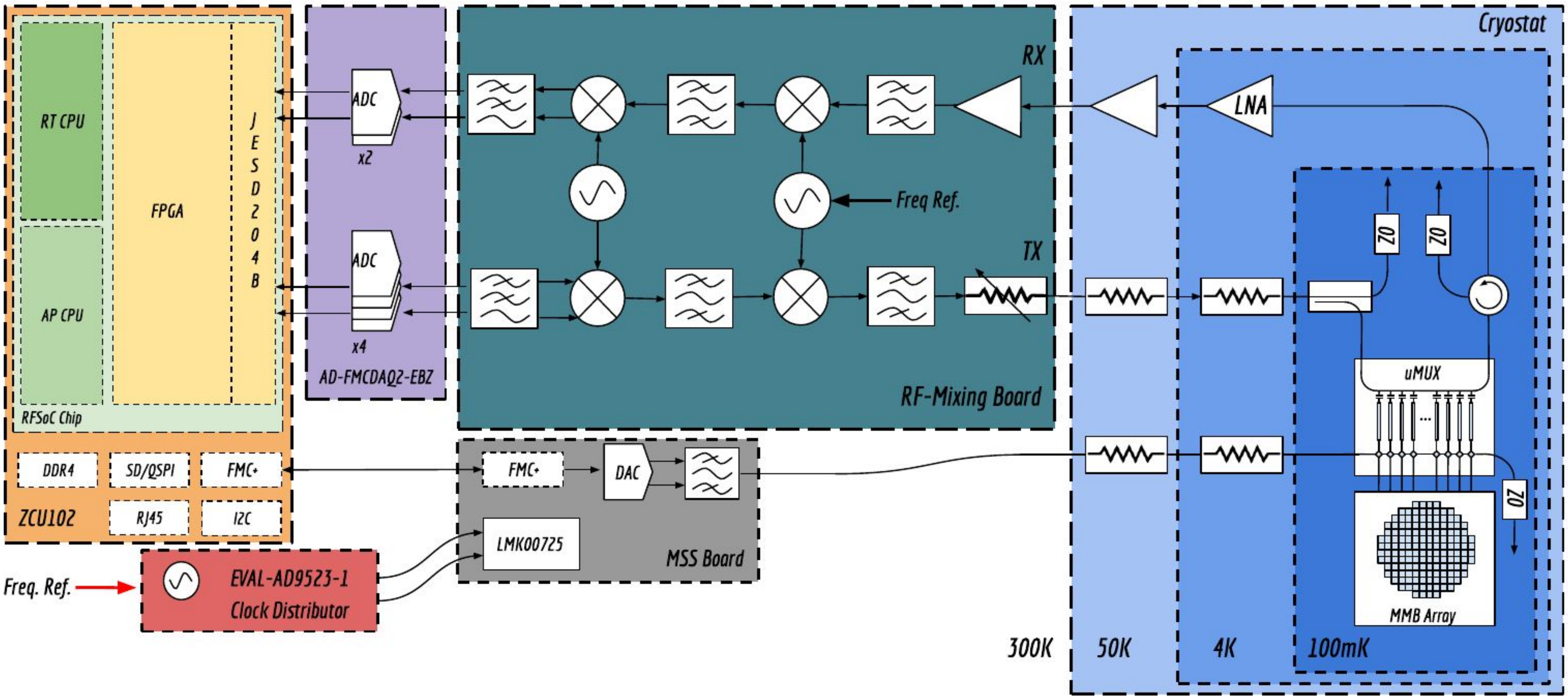

Background noise

Center frequency

$$\mathrm{NEP}_{\gamma}^{2} = 2hf\,P_{\mathrm{opt}} + \frac{2P_{\mathrm{opt}}^{2}}{m\Delta f}$$

Signal power
absorber by the MMB

Bandwidth

MMB noise

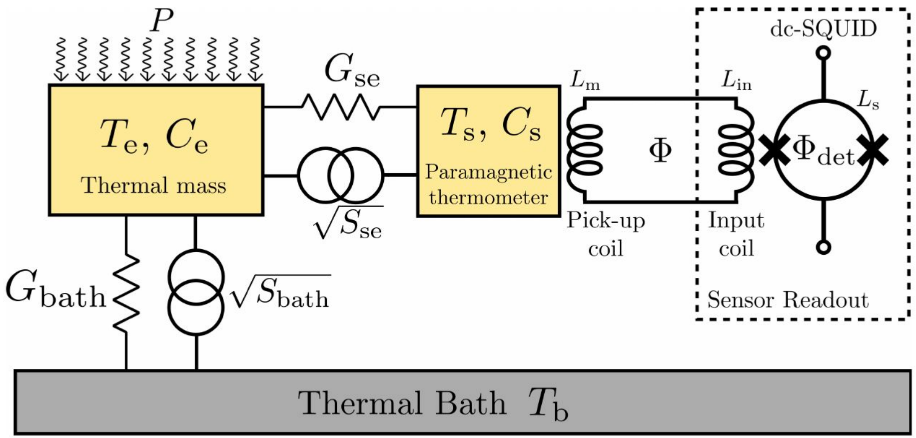

P
G_{se}
T_e, C_e
Thermal mass
T_s, C_s
Paramagnetic thermometer
$\sqrt{S_{se}}$
L_m
Φ
Pick-up coil
L_{in}
Input coil
dc-SQUID
L_s
Φ_{det}
Sensor Readout
G_{bath}
$\sqrt{S_{bath}}$
Thermal Bath T_b

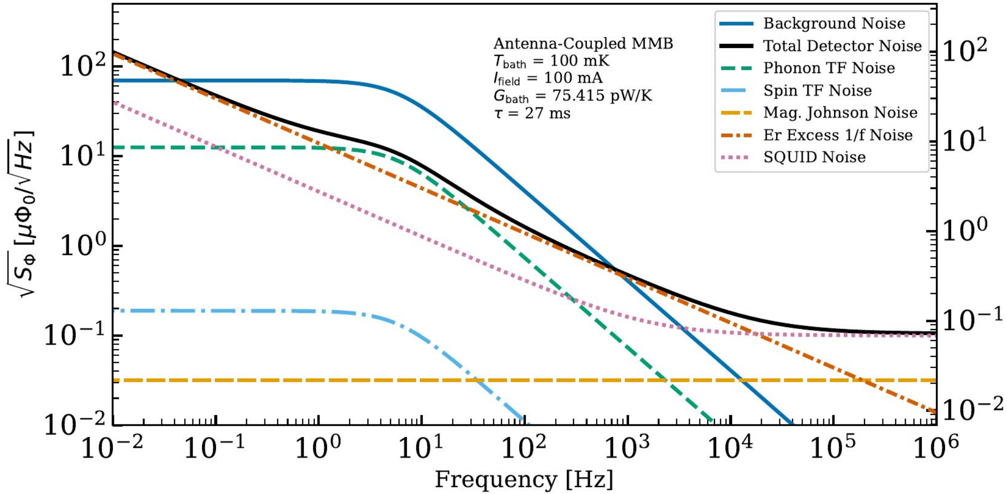

Antenna-Coupled MMB
T_{bath} = 100 mK
I_{field} = 100 mA
G_{bath} = 75.415 pW/K
τ = 27 ms
Background Noise
Total Detector Noise
Phonon TF Noise
Spin TF Noise
Mag. Johnson Noise
Er Excess 1/f Noise
SQUID Noise
$\sqrt{S_\Phi}$ [$\mu\Phi_0/\sqrt{Hz}$]
Frequency [Hz]

MSS: Noise analysis

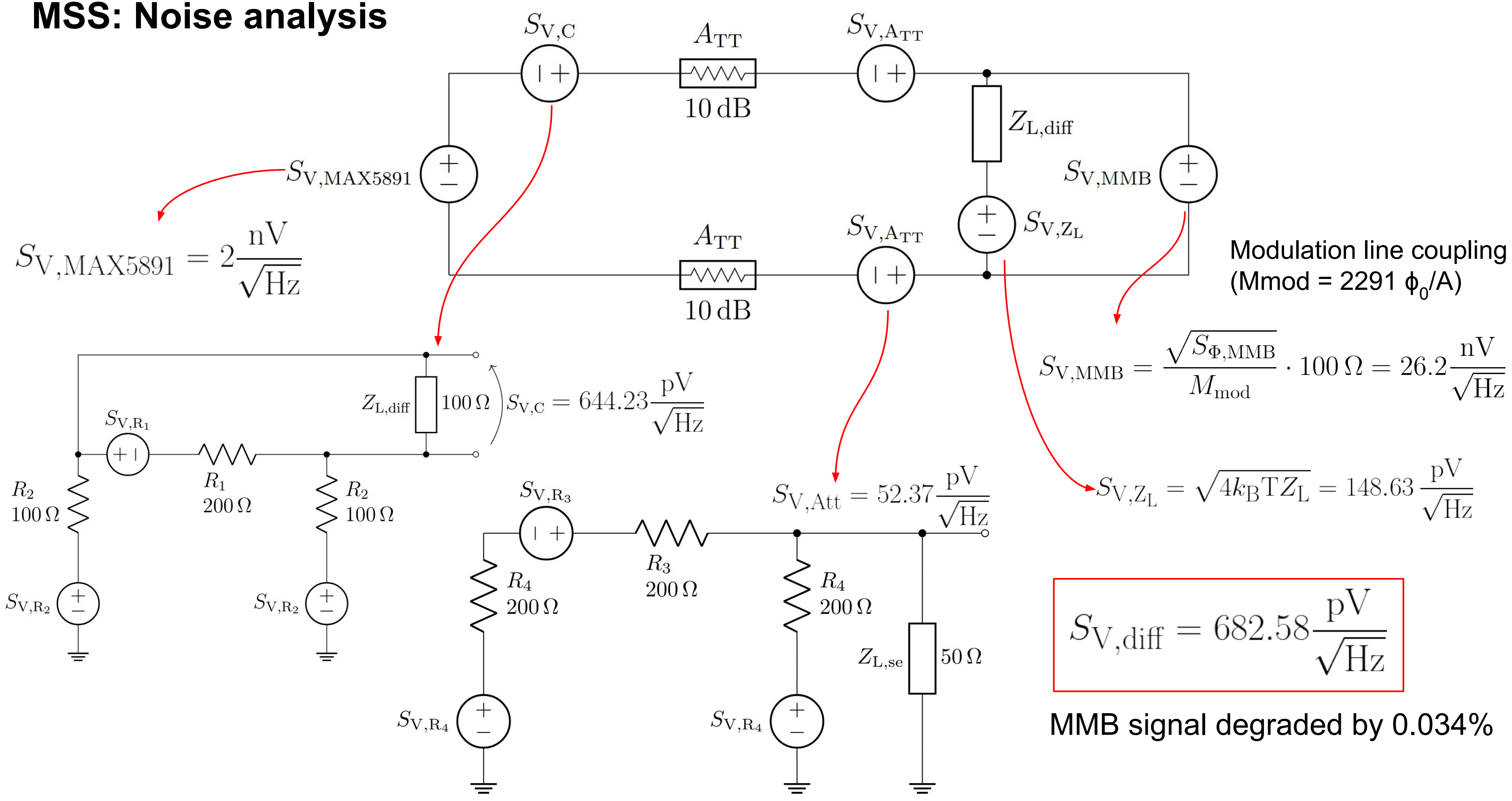

$$S_{V,MAX5891} = 2\frac{nV}{\sqrt{Hz}}$$

$$S_{V,C} = 644.23\frac{pV}{\sqrt{Hz}}$$

$$S_{V,Att} = 52.37\frac{pV}{\sqrt{Hz}}$$

Modulation line coupling (Mmod = 2291 ϕ_0/A)

$$S_{V,MMB} = \frac{\sqrt{S_{\Phi,MMB}}}{M_{mod}} \cdot 100\,\Omega = 26.2\frac{nV}{\sqrt{Hz}}$$

$$S_{V,Z_L} = \sqrt{4k_B T Z_L} = 148.63\,\frac{pV}{\sqrt{Hz}}$$

$$S_{V,diff} = 682.58\frac{pV}{\sqrt{Hz}}$$

MMB signal degraded by 0.034%

MSS digital backend

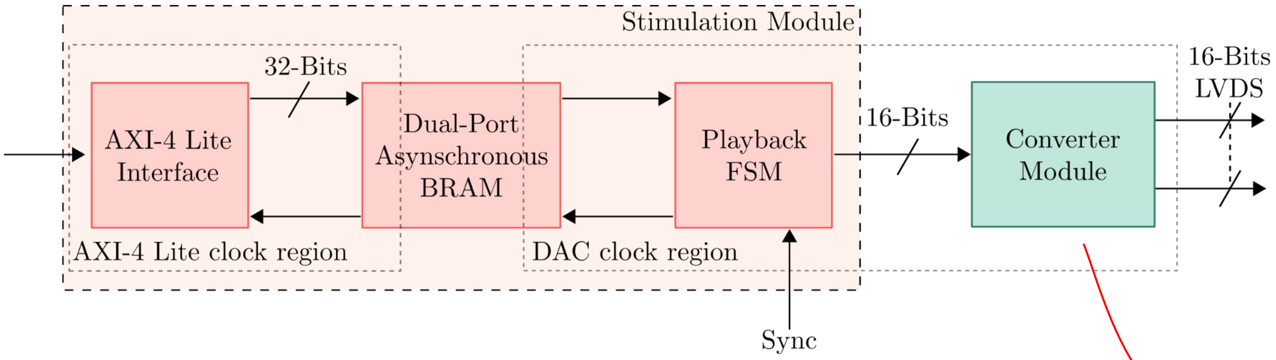

ZCU102

- ➔ ZCU102 selected as digital backend
- ➔ Dual-port BRAM
  - ◆ Arbitrary waveform generation
  - ◆ Playback continuous signal
  - ◆ Real-time configuration using AXI-Lite protocol
- ➔ Synthesizable signal frequencies

$$\frac{f_{\text{clk}}}{\text{L}_{\text{bram}}} \geq f_{\text{out}} > \frac{f_{\text{clk}}}{2}$$

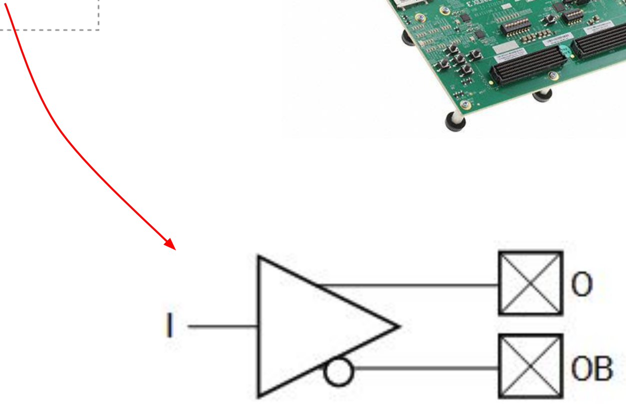

Differential Signaling Output Buffer

MSS characterization using oscilloscope DPO 7104

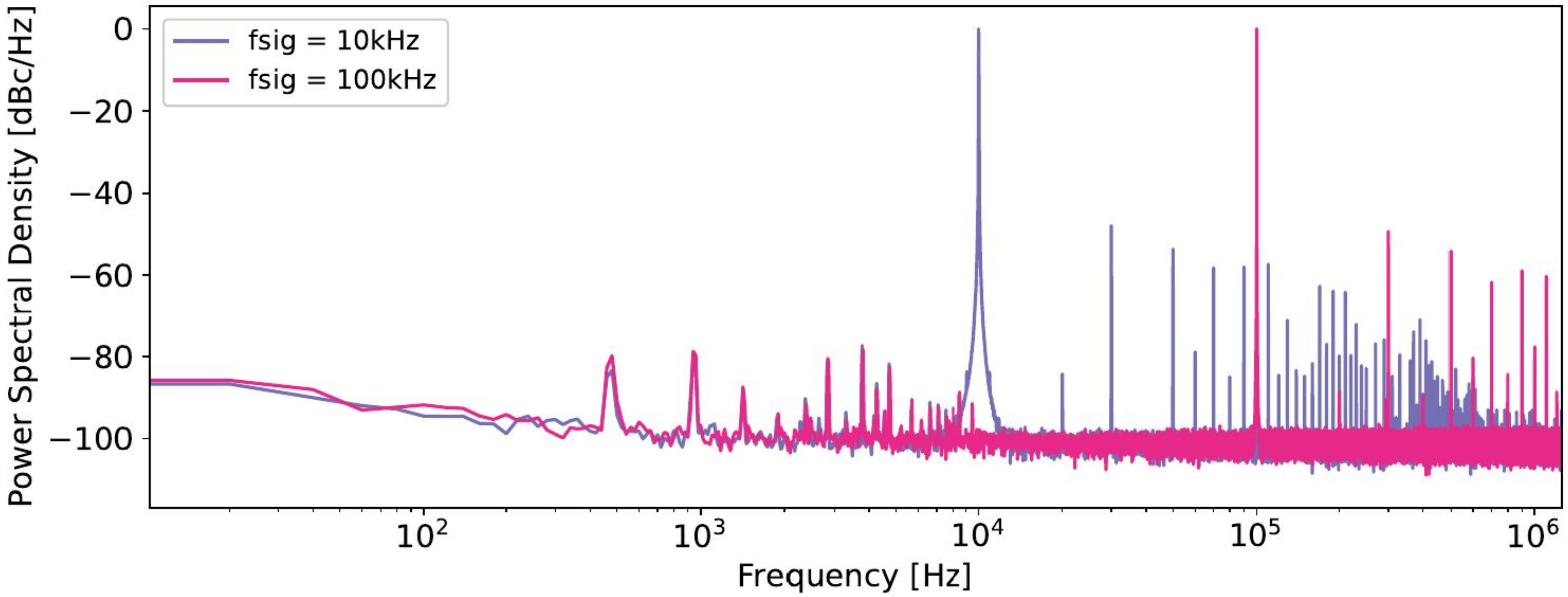

Red Pitaya baseline

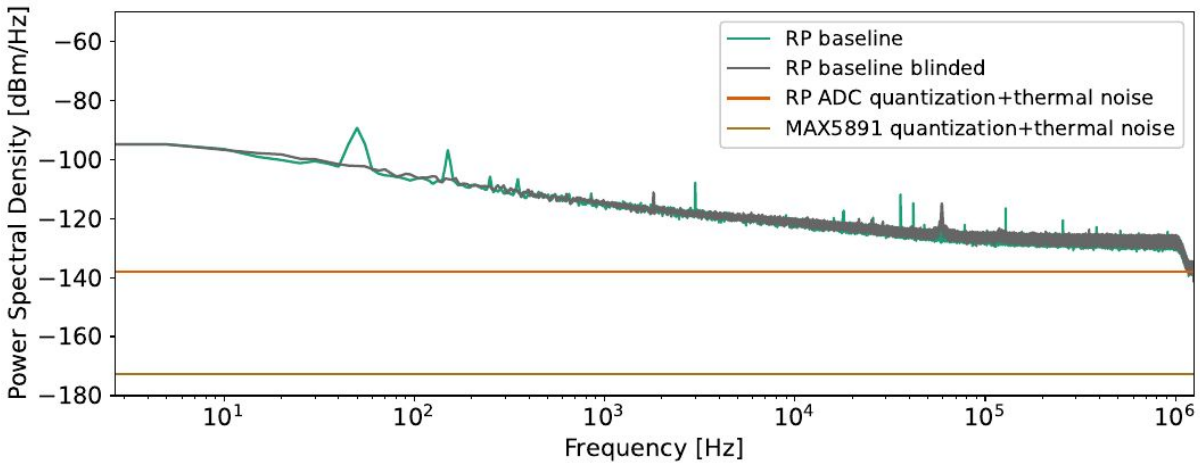

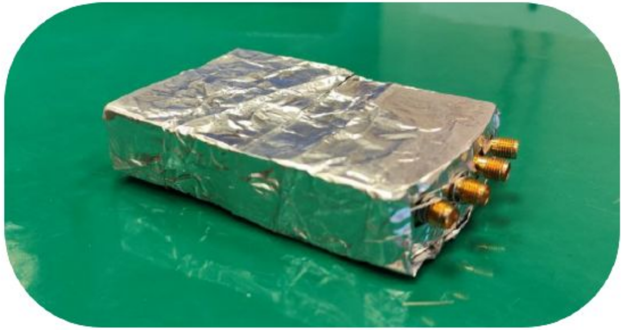

Down-conversion implementation

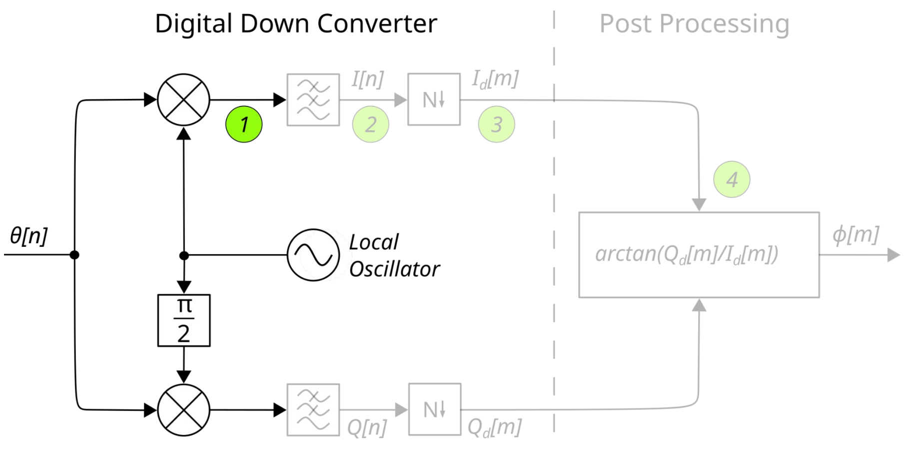

1 Down-conversion

- ➔ DSP slice for efficient multiplication
- ➔ Complex signal generated by a DDS
- ➔ A phase value is generated as the index for a memory preloaded with sine and cosine samples
- ➔ The phase value is generated by cyclically adding the Phase Register value to the Phase Accumulator
- ➔ θ_0 sets the initial phase
- ➔ One phase register for each input signal to be multiplexed in time

Direct Digital Synthesizer

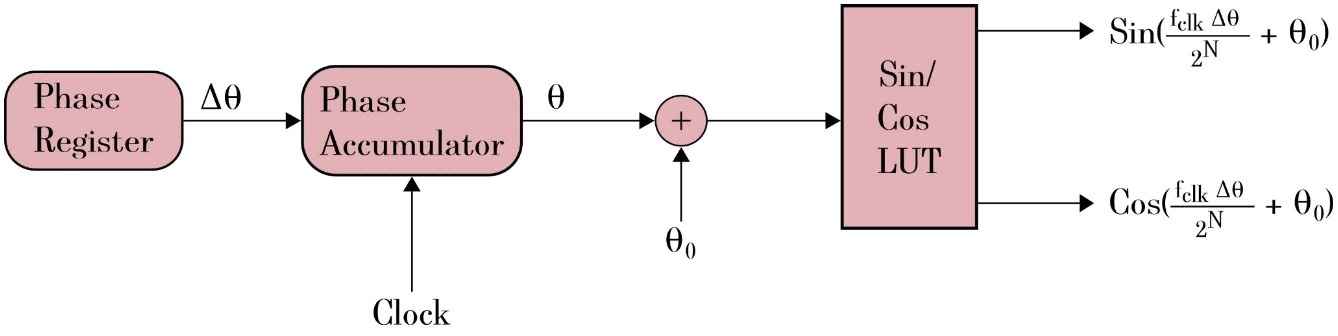

Multiplication implementation

1 Multiplier

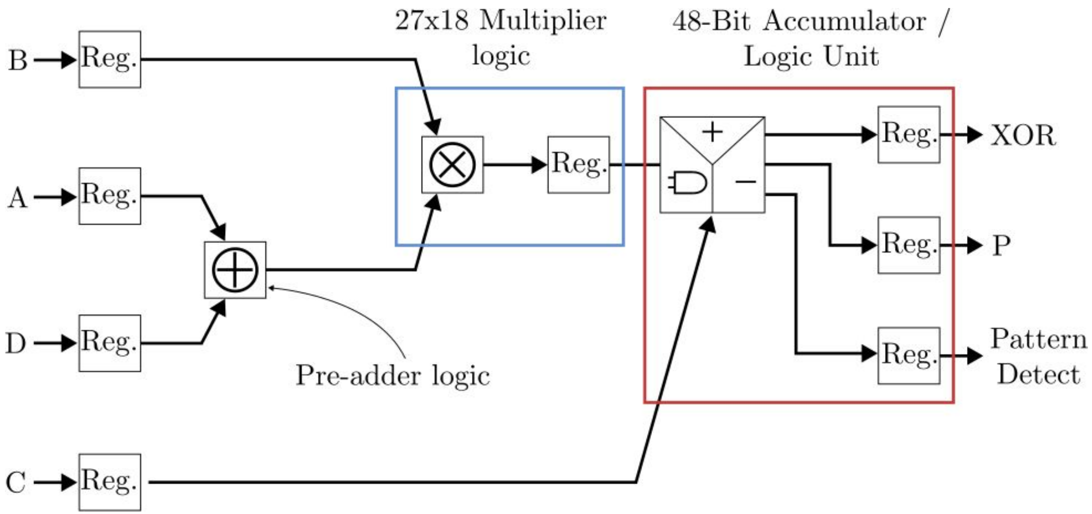

- ➔ Intellectual Property Core DSP48E2
- ➔ Specialized block for efficient multiplication and accumulation (MAC operations)

Arctan implementation

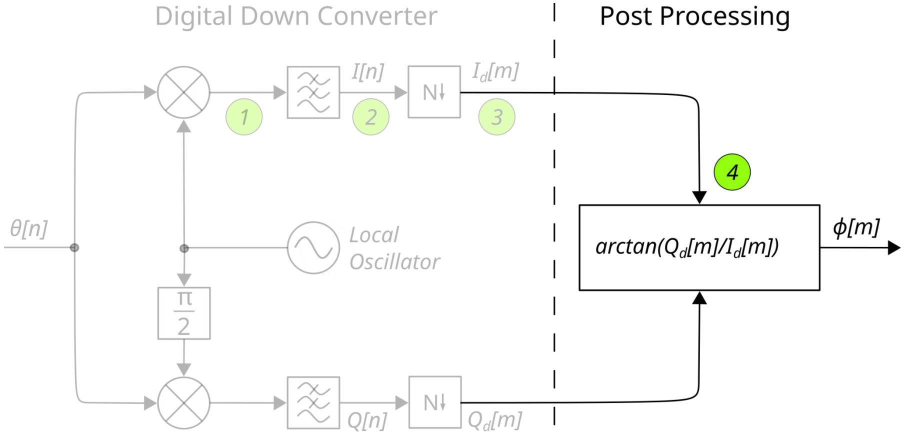

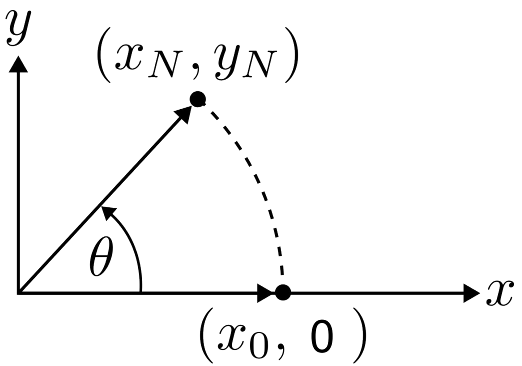

$$x[n+1] = x[n] - d[n] \cdot 2^{-n} \cdot y[n]$$
$$y[n+1] = y[n] - d[n] \cdot 2^{-n} \cdot x[n]$$

4 CORDIC algorithm

- ➔ Hardware efficient: requires only additions, subtractions and binary shifts
- ➔ A starting vector (x_0, 0) is iteratively rotated to the angle corresponding to arctan(y_N/x_N)
- ➔ The accumulated sum of the rotated angles provides the final result for the arctangent
- ➔ Adjustable precision: number of iterations determines the precision of the result

Aliasing effect mitigation in a measurement

$$\phi'[m] = \phi[m] + c + \sum_{l=1}^{\infty} (-1)^l \frac{b^l}{l} \frac{\partial^l \phi'[m]}{\partial b^l}\bigg|_{(b=0)}$$

$$= \phi[m] + c + \sum_{l=1}^{\infty} (-1)^l \frac{b^l}{l} \cdot \sin((2\Omega_{det} m + c - d)l)$$

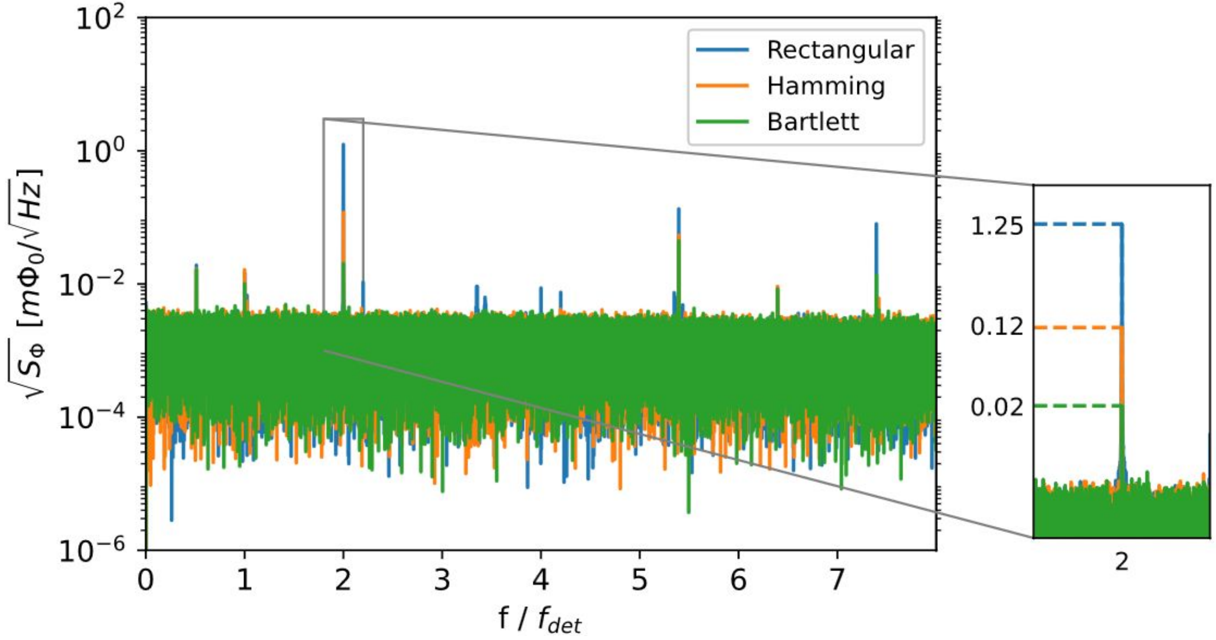

Fluxramp demodulator with phase delay

$$\Phi_{\text{det}}(t) + \Phi_0(t) = \arctan\left(-\frac{\int_{T_{\text{ramp}}} \theta(t+t_0)\ \sin(\omega_{mod}t)dt}{\int_{T_{\text{ramp}}} \theta(t+t_0)\ \cos(\omega_{mod}t)dt}\right)\frac{\Phi_0}{2\pi}$$

Fluxramp demodulator implementation

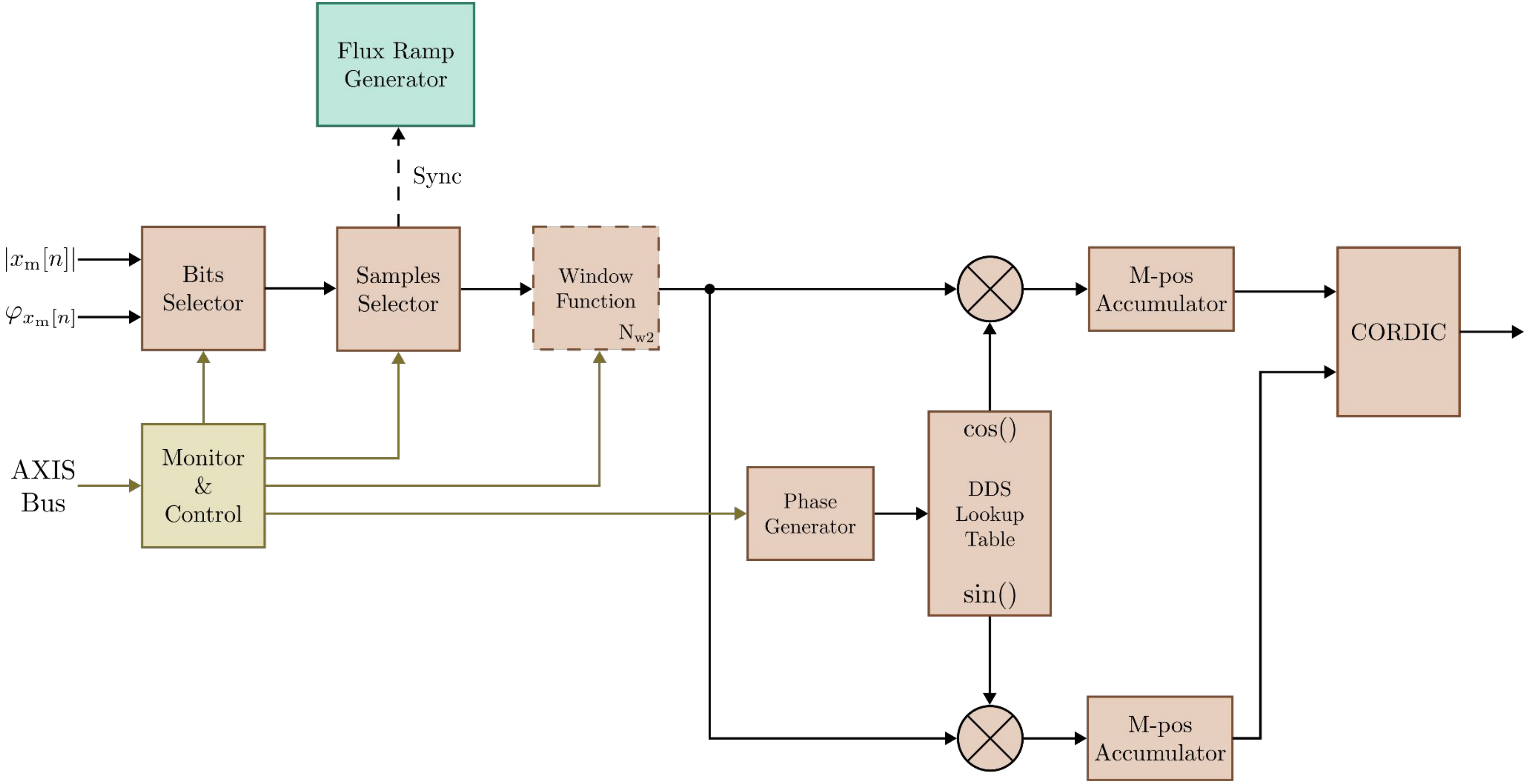

Digital backend

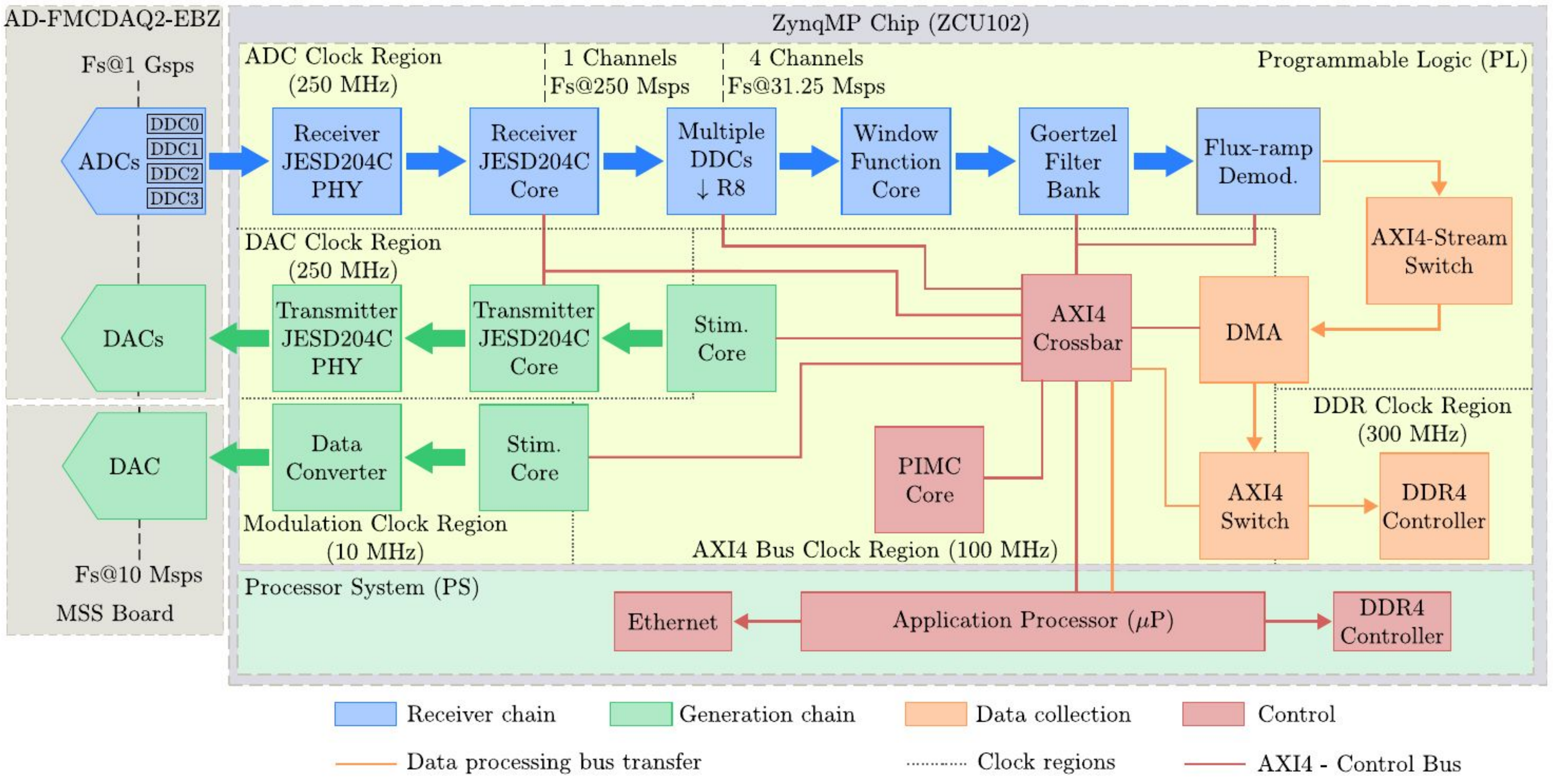

Frequency planning of the digital processing chain

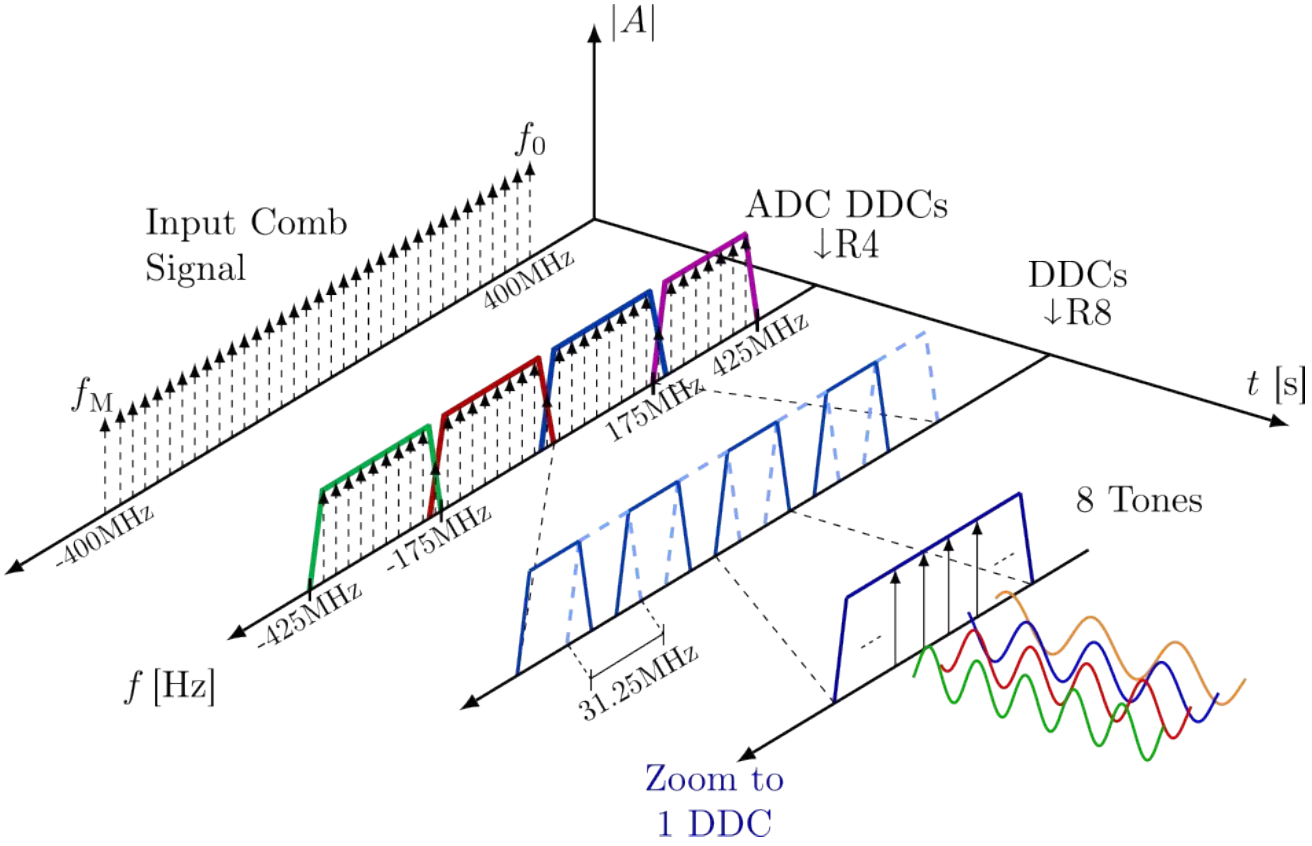

Readout signal processing system

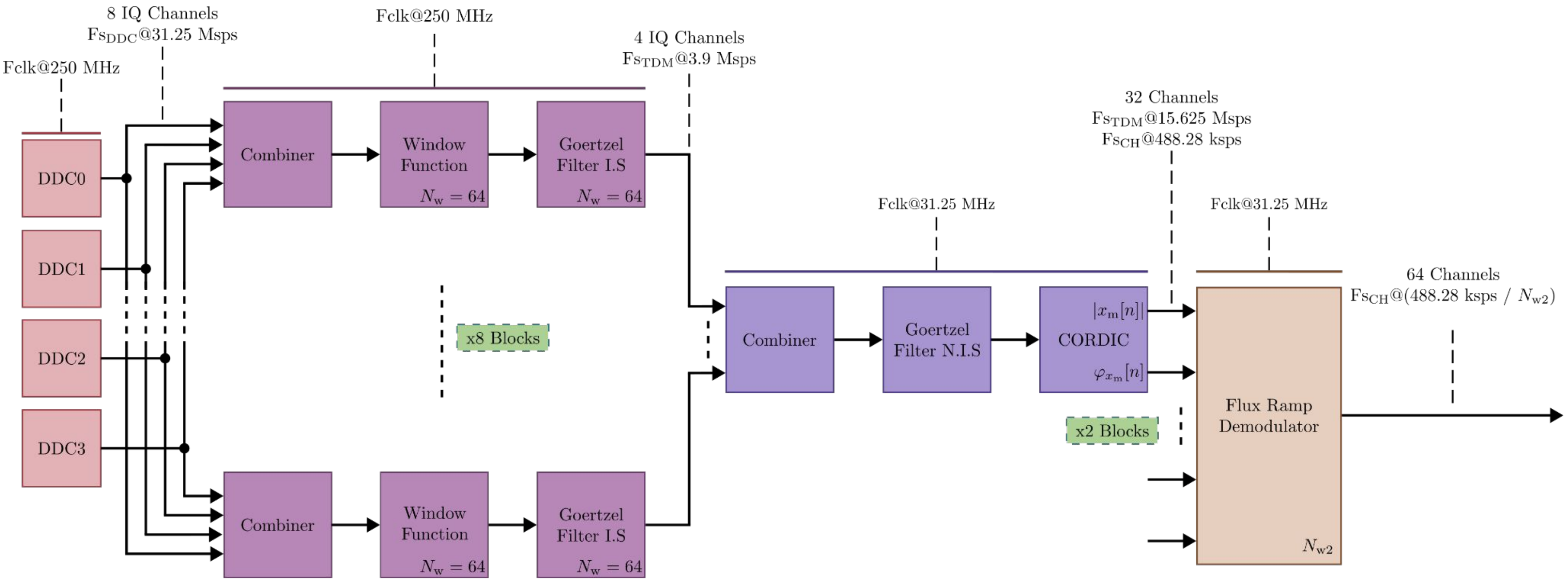

System resources for 2048 detectors

				Resources															
	Module	Description	N channels	Logic LUT	Mem LUT	FF Regs	FF latch	CARRY8	F7 MUX	F8 MUX	F9 MUX	BRAM B36/FIFO	BRAM B18	DSPs	I/O	CLK BUFFs	PLL	MMCM	GTH
Generation	stimulation	*Fluxramp signal*	-	0,19	0,00	0,11	0,00	0,01	0,00	0,00	0,00	3,51	0,00	0,00	0,00	0,00	0,00	0,00	0,00
	bit_to_lvds	*Fluxramp conditioning*	-	0,00	0,00	0,00	0,00	0,00	0,00	0,00	0,00	0,00	0,00	0,00	9,76	0,00	0,00	0,00	0,00
	stimulation	*Readout signal*	-	0,23	0,00	0,13	0,00	0,01	0,00	0,00	0,00	14,04	0,00	0,00	0,00	0,00	0,00	0,00	0,00
	jesd204phy	*Readout signal tx/rx interface*	-	1,06	0,00	0,70	0,00	0,43	0,01	0,01	0,00	0,00	0,00	0,00	0,00	1,98	0,00	0,00	16,67
	jesd204tx	*Readout signal tx interface*	-	0,72	0,03	0,31	0,00	0,01	0,01	0,01	0,00	0,00	0,00	0,00	0,00	0,00	0,00	0,00	0,00
	sample_mapper_dac		-	0,00	0,00	0,00	0,00	0,00	0,00	0,00	0,00	0,00	0,00	0,00	0,00	0,00	0,00	0,00	0,00
		Subtotal		**2,20**	**0,03**	**1,25**	**0,00**	**0,46**	**0,02**	**0,02**	**0,00**	**17,55**	**0,00**	**0,00**	**9,76**	**1,98**	**0,00**	**0,00**	**16,67**
Processing	jesd204rx	*Readout signal rx interface*	-	1,25	0,47	0,63	0,00	0,24	0,02	0,02	0,00	0,00	0,00	0,00	0,00	0,00	0,00	0,00	0,00
	sample_mapper_adc		-	0,00	0,00	0,00	0,00	0,00	0,00	0,00	0,00	0,00	0,00	0,00	0,00	0,00	0,00	0,00	0,00
	sample_mapper_adc		-	0,00	0,00	0,00	0,00	0,00	0,00	0,00	0,00	0,00	0,00	0,00	0,00	0,00	0,00	0,00	0,00
	sample_splitter	DDC input	32	0,00	0,00	0,00	0,00	0,00	0,00	0,00	0,00	0,00	0,00	0,00	0,00	0,00	0,00	0,00	0,00
	axi_ddc_controller	*DDC Controler*	32	0,03	0,00	0,07	0,00	0,00	0,00	0,00	0,00	0,00	0,00	0,00	0,00	0,00	0,00	0,00	0,00
	ga_ddc	*DDC0*	8	0,50	0,54	0,56	0,00	0,42	0,00	0,00	0,00	0,22	0,00	0,75	0,00	0,00	0,00	0,00	0,00
	ga_ddc	*DDC1*	8	0,50	0,54	0,56	0,00	0,42	0,00	0,00	0,00	0,22	0,00	0,75	0,00	0,00	0,00	0,00	0,00
	ga_ddc	*DDC2*	8	0,50	0,54	0,56	0,00	0,42	0,00	0,00	0,00	0,22	0,00	0,75	0,00	0,00	0,00	0,00	0,00
	ga_ddc	*DDC3*	8	0,50	0,54	0,56	0,00	0,42	0,00	0,00	0,00	0,22	0,00	0,75	0,00	0,00	0,00	0,00	0,00
	sample_combiner	DDC combiner	32	0,02	0,00	0,02	0,00	0,00	0,00	0,00	0,00	0,00	0,00	0,00	0,00	0,00	0,00	0,00	0,00
	multiplier_array	*GA window multiplier*	4	0,02	0,01	0,03	0,00	0,04	0,00	0,00	0,00	0,00	0,00	0,08	0,00	0,00	0,00	0,00	0,00
	win_store	*GA window*	4	0,01	0,00	0,01	0,00	0,00	0,00	0,00	0,00	0,44	0,00	0,00	0,00	0,00	0,00	0,00	0,00
	axi_win_function		4																
	gaka_controller	*GA controller*	4	0,03	0,00	0,08	0,00	0,00	0,00	0,00	0,00	0,00	0,00	0,00	0,00	0,00	0,00	0,00	0,00
	gaka	*GA*	4	0,10	0,07	0,11	0,00	0,05	0,00	0,00	0,00	0,00	0,00	0,08	0,00	0,00	0,00	0,00	0,00
	mag_phase_processor	*GA mag and phase gen*	32	1,67	0,10	0,87	0,00	1,58	0,00	0,00	0,00	0,00	0,00	0,63	0,00	0,00	0,00	0,00	0,00
	parallel_decimator	GA	4	0,07	0,00	0,05	0,00	0,08	0,00	0,00	0,00	0,00	0,00	0,00	0,00	0,00	0,00	0,00	0,00
	parallel_decimator	GA	4	0,07	0,00	0,05	0,00	0,08	0,00	0,00	0,00	0,00	0,00	0,00	0,00	0,00	0,00	0,00	0,00
	serializer	*GA serializer*	4	0,01	0,00	0,02	0,00	0,01	0,00	0,00	0,00	0,00	0,00	0,00	0,00	0,00	0,00	0,00	0,00
	fluxramp_demodulation	*Fluxramp demodulator*	32	1,59	0,02	0,86	0,01	1,42	0,00	0,00	0,00	0,77	0,05	0,08	0,00	0,00	0,00	0,00	0,00
		Subtotal		**225,09**	**93,59**	**206,39**	**0,16**	**193,84**	**0,02**	**0,02**	**0**	**153,12**	**0,8**	**158,4**	**0**	**0**	**0**	**0**	**0**
Clock Managers	clk_wiz	*Clock Wizzard Fluxramp*		0,00	0,00	0,00	0,00	0,00	0,00	0,00	0,00	0,00	0,00	0,00	0,61	0,50	0,00	25,00	0,00
	utils_ds_buf	*Clock buffer*		0,00	0,00	0,00	0,00	0,00	0,00	0,00	0,00	0,00	0,00	0,00	0,00	0,25	0,00	0,00	0,00
	clk_wiz	*Clock Wizzard 250 MHz*		0,00	0,00	0,00	0,00	0,00	0,00	0,00	0,00	0,00	0,00	0,00	0,00	0,99	0,00	25,00	0,00
	utils_ds_buf	Clock buffer		0	0	0	0	0	0	0	0	0	0	0	0	0,25	0	0	0
	DDR4			3,27	0,41	2,11	0	0,17	0,12	0	0	2,74	0,05	0,12	15,55	1,98	12,5	25	0
	XBAR			0,14	0	0,03	0	0	0	0	0	0	0	0	0	0	0	0	0
		Subtotal		**3,41**	**0,41**	**2,14**	**0**	**0,17**	**0,12**	**0**	**0**	**2,74**	**0,05**	**0,12**	**16,16**	**3,97**	**12,5**	**75**	**0**
Data access	dma_controller			0,75	0,09	0,56	0,00	0,13	0,00	0,00	0,00	6,80	0,11	0,00	0,00	0,00	0,00	0,00	0,00
	dma_axis_register			0,01	0,00	0,02	0,00	0,00	0,00	0,00	0,00	0,00	0,00	0,00	0,00	0,00	0,00	0,00	0,00
	axis_channel_select			0,01	0,00	0,03	0,00	0,00	0,00	0,00	0,00	0,00	0,00	0,00	0,00	0,00	0,00	0,00	0,00
		Subtotal		**0,77**	**0,09**	**0,61**	**0**	**0,13**	**0**	**0**	**0**	**6,8**	**0,11**	**0**	**0**	**0**	**0**	**0**	**0**
Miscellaneuos	zynqmp	*Microprocesador interface*		0,14	0,00	0,01	0,00	0,00	0,00	0,00	0,00	0,00	0,00	0,00	0,00	0,50	0,00	0,00	0,00
	global_reset			0,00	0,00	0,00	0,00	0,00	0,00	0,00	0,00	0,00	0,00	0,00	0,00	0,00	0,00	0,00	0,00
		Subtotal		**0,14**	**0**	**0,01**	**0**	**0**	**0**	**0**	**0**	**0**	**0**	**0**	**0**	**0,5**	**0**	**0**	**0**
	Total		**2048**	**231,61**	**94,12**	**210,40**	**0,16**	**194,60**	**0,16**	**0,04**	**0,00**	**180,21**	**0,96**	**158,52**	**25,92**	**6,45**	**12,50**	**75,00**	**16,67**

Spectral Engineering results

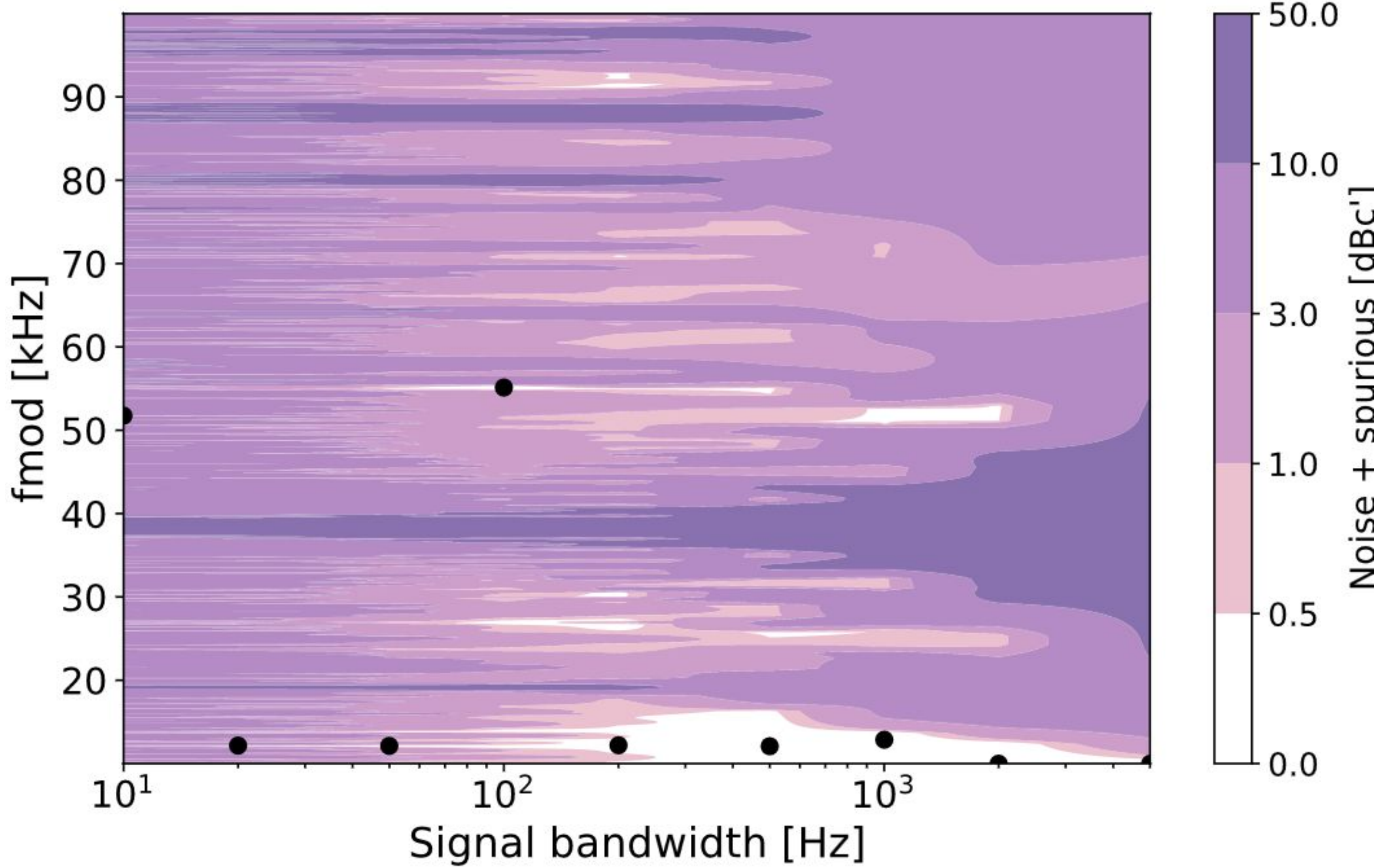

µMUX characterization

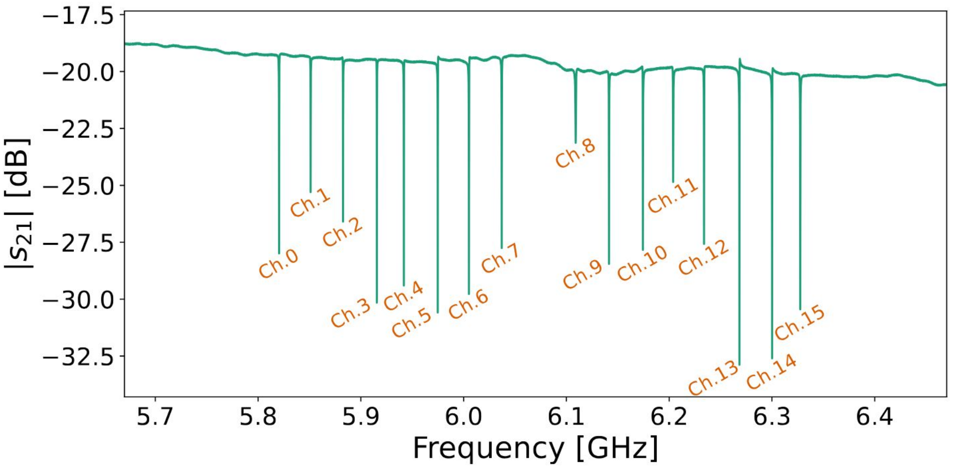

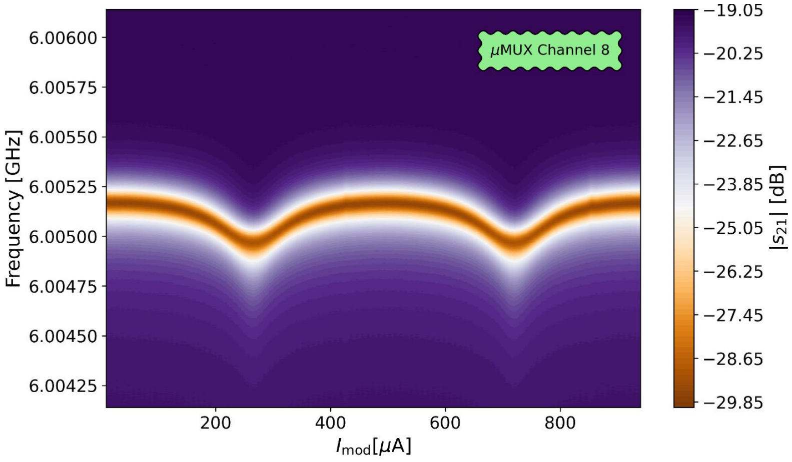

- ➔ µMUX channel measurement using commercial VNA and no modulation signal
- ➔ Obtained channel parameters:
  - ◆ Resonance frequencies
  - ◆ Bandwidths
  - ◆ Transmission depths

- ➔ Adding a DC current to the modulation line
- ➔ Swept over two SQUID periods
- ➔ Resonator response as a function of the flux signal
- ➔ Mmod calculated

Cryogenic setup

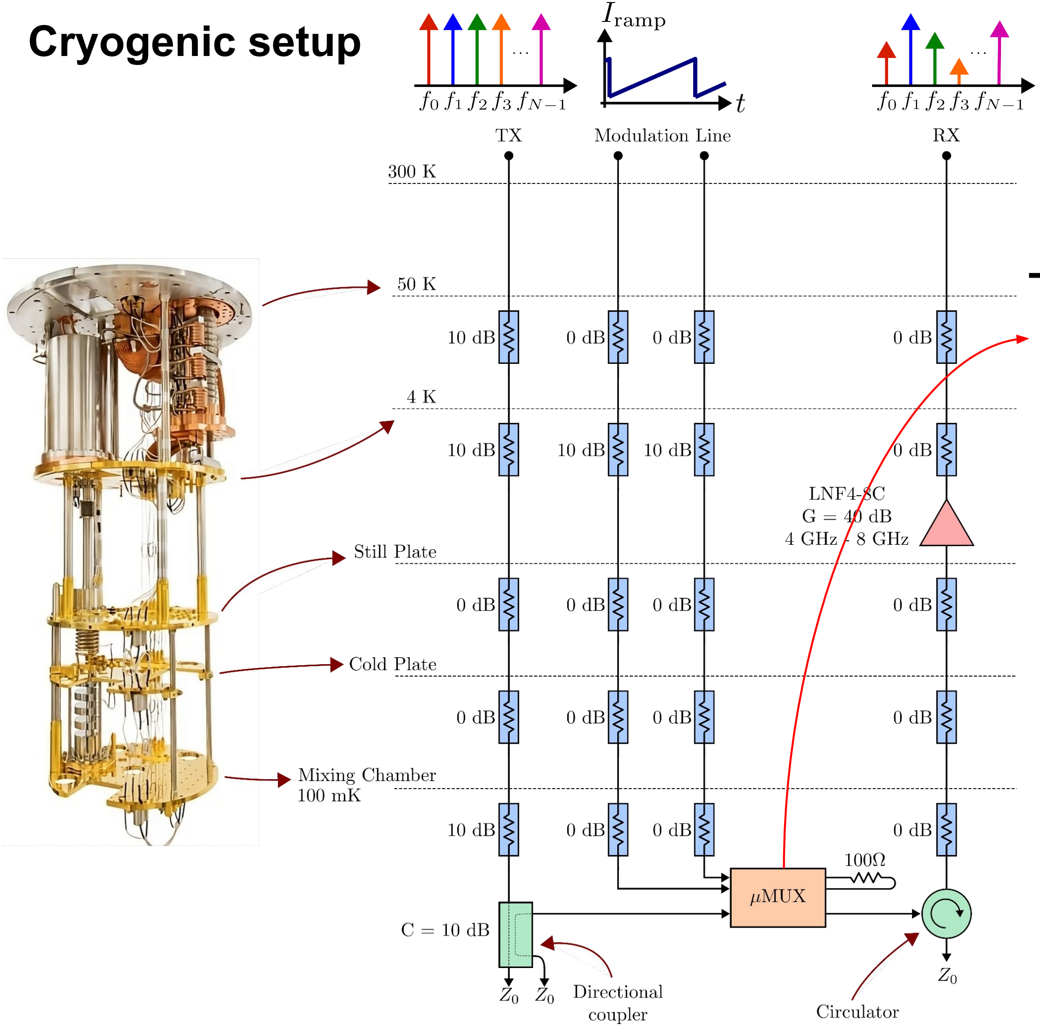

Microwave SQUID Multiplexer

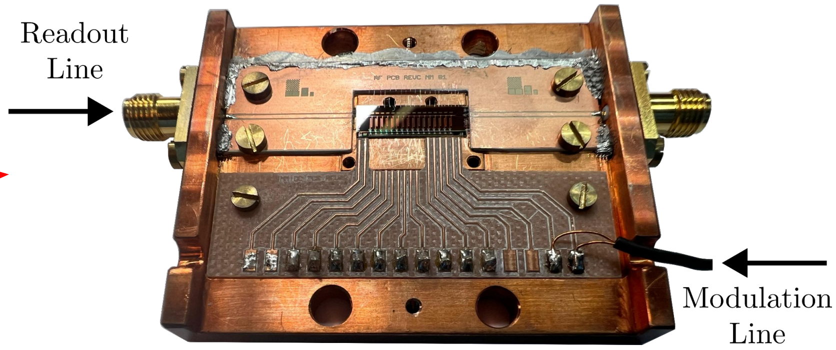

- ➔ Cryostat to cooldown at sub-K temperatures
- ➔ 16-ch Microwave SQUID Multiplexer located at 100mK
- ➔ Readout signal attenuation to achieve -70dBm μMUX measurement
- ➔ The readout signal is amplified on the return path for optimal acquisition
- ➔ Differential fluxramp signal chain

Microwave SQUID Multiplexer parameters

	Ch. 5	Ch. 6	Ch. 7	Ch. 8
$\lvert s_{21}^{\mathrm{min}}\rvert$ [dB]	-30.55	-29.84	-31.2	-29.9
$f_{\mathrm{r},0}$ [GHz]	5.915534	5.941953	5.974811	6.005102
$f_{\mathrm{r,min}}$ [GHz]	5.915452	5.941858	5.974705	6.004965
$f_{\mathrm{r,max}}$ [GHz]	5.915596	5.942019	5.97488	6.005169
$\Delta f_{\mathrm{r}}^{\mathrm{pp}}$ [kHz]	143.72	160.26	174.42	204.2
BW_{res} [kHz]	175	216.46	220.8	267.36
η	0.82	0.74	0.79	0.764
Q_{l}	33795	27450	27059	22460

Optimal µMUX measurement conditions

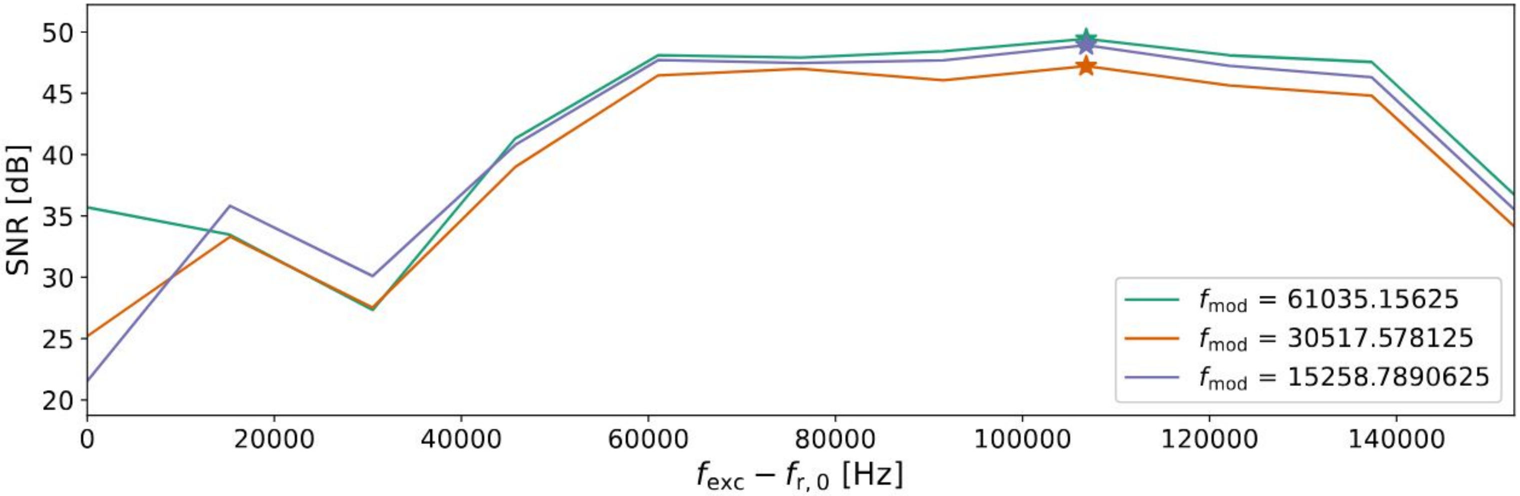

Open-loop noise